

Novel furan-2-yl-1H-pyrazoles possess inhibitory activity against α -synuclein aggregation

Philip Ryan, Mingming Xu, Kousar Jahan, Andrew K. Davey, Prasad V. Bharatam, Shailendra Anoopkumar-Dukie, Michael Kassiou, George D Mellick, and Santosh RUDRAWAR

ACS Chem. Neurosci., **Just Accepted Manuscript** • DOI: 10.1021/acscchemneuro.0c00252 • Publication Date (Web): 18 Jun 2020

Downloaded from pubs.acs.org on June 29, 2020

Just Accepted

“Just Accepted” manuscripts have been peer-reviewed and accepted for publication. They are posted online prior to technical editing, formatting for publication and author proofing. The American Chemical Society provides “Just Accepted” as a service to the research community to expedite the dissemination of scientific material as soon as possible after acceptance. “Just Accepted” manuscripts appear in full in PDF format accompanied by an HTML abstract. “Just Accepted” manuscripts have been fully peer reviewed, but should not be considered the official version of record. They are citable by the Digital Object Identifier (DOI®). “Just Accepted” is an optional service offered to authors. Therefore, the “Just Accepted” Web site may not include all articles that will be published in the journal. After a manuscript is technically edited and formatted, it will be removed from the “Just Accepted” Web site and published as an ASAP article. Note that technical editing may introduce minor changes to the manuscript text and/or graphics which could affect content, and all legal disclaimers and ethical guidelines that apply to the journal pertain. ACS cannot be held responsible for errors or consequences arising from the use of information contained in these “Just Accepted” manuscripts.

1
2
3 ACS CHEMICAL NEUROSCIENCE MANUSCRIPT:
4
5

6
7 **Novel furan-2-yl-1*H*-pyrazoles possess inhibitory activity**
8 **against α -synuclein aggregation**
9

10
11
12
13 Philip Ryan^{1,2,3}, Mingming Xu⁴, Kousar Jahan⁵, Andrew K. Davey^{1,2,3}, Prasad V. Bharatam⁵,
14 Shailendra Anoopkumar-Dukie^{1,2}, Michael Kassiou⁶, George D. Mellick^{4†}, Santosh
15 Rudrawar^{1,2,3,†}
16

17 ¹*School of Pharmacy and Pharmacology, Griffith University, Gold Coast, QLD 4222, Australia.*

18 ²*Quality Use of Medicines Network, Griffith University, Gold Coast, QLD 4222, Australia.*

19 ³*Menzies Health Institute Queensland, Griffith University, Gold Coast, QLD 4222, Australia*

20 ⁴*Griffith Institute for Drug Discovery, Griffith University, Nathan, QLD 4111, Australia.*

21 ⁵*National Institute of Pharmaceutical Education and Research (NIPER) SAS Nagar, 160062, India*

22 ⁶*School of Chemistry, The University of Sydney, NSW 2006, Australia.*
23
24
25
26
27
28
29

30 †**Corresponding authors:**

31 1) Dr Santosh Rudrawar

E-mail address: s.rudrawar@griffith.edu.au

32 2) Prof George Mellick

E-mail address: g.mellick@griffith.edu.au
33
34
35
36
37
38
39
40
41
42
43
44
45
46
47
48
49
50
51
52
53
54
55
56
57
58
59
60

1
2
3 **Abstract:** A series of novel furan-2-yl-1*H*-pyrazoles and their chemical precursors were
4 synthesised and evaluated for their effectiveness at disrupting α -synuclein (α -syn) aggregation
5 *in vitro*. The compounds were found to inhibit α -syn aggregation with efficacy comparable to
6 the promising drug candidate anle138b. The results of this study indicate that compounds **8b**,
7 **8l** and **9f** may qualify as secondary leads for the structure-activity relationship studies aimed
8 to identify the suitable compounds for improving the modulatory activity targeted at α -syn
9 self-assembly related to Parkinson's disease.
10
11
12
13
14
15
16
17
18

19 **Keywords:** α -Synuclein aggregation; Parkinson's disease; neurodegenerative diseases;
20 anle138b; Molecular modelling studies; aminopyrazole.
21
22
23
24
25
26
27
28
29
30
31
32
33
34
35
36
37
38
39
40
41
42
43
44
45
46
47
48
49
50
51
52
53
54
55
56
57
58
59
60

INTRODUCTION

Neurodegenerative diseases (NDs) are causing significant increase in the societal burden, with their growing prevalence of cases in aged population. Though symptoms can be treated for some NDs, there are no therapies that address the underlying progressive, disease-related processes. Various novel strategies have been pursued towards the diagnosis and treatment of NDs such as Alzheimer's disease (AD) and Parkinson's disease (PD). A number of proteopathic NDs share common defining characteristics, specifically the misfolding and self-assembly of the culprit proteins at the molecular level leading to the accretion and propagation of toxic soluble species and the appearance of insoluble fibrillar structures.¹ Ultimately these prion-like processes lead to the neuronal cell death and the onset of symptoms.

Regarding AD and PD, mounting evidence indicates that the pathogenesis is associated with the arrival of soluble, oligomeric protein complexes, rather than the consequential fibrillar deposits.² Therefore, modern therapeutic approaches aim to arrest oligomer formation, and related processes, rather than targeting the larger aggregate structures.³ Recently, the diphenylpyrazole anle138b (**1**, **Figure 1**) was identified as a potent modulator of protein oligomerisation.⁴ It displays potent antiprion activity with high CNS bioavailability and low cytotoxicity, even able to prolong survival in prion-infected mice.⁴ The compound **1** is also able to inhibit the formation and accumulation of α -synuclein (α -syn) oligomers in the brain, reduce PD-associated motor deficits and prolong the survival of various animal models of PD.⁴ ⁵ In addition, anle138b effectively bind to the aggregated tau and inhibit tau aggregation. It also possesses a tendency to ameliorate AD symptoms, and increases survival time and improve cognition in treated transgenic PS19 mice.⁶ When administered orally, anle138b ameliorates A β -induced deficits in synaptic plasticity and memory formation in the APPPS1 Δ E9 mouse model for amyloid pathology.⁷ Finally, oral administration of anle138b in Multiple System Atrophy (MSA) model mice reverses impaired motor function; reduces levels of α -syn oligomers and glial cytoplasmic inclusions; and results in the preservation of dopaminergic neurons and reduction of microglial activation in the *substantia nigra*.⁵ The compound **1** is undergoing pre-clinical development for use as a PD therapeutic agent, and has been recommended for use in clinical trials for MSA and AD.^{6, 8}

Reports suggest that compound **1** modulates the oligomer formation by targeting structure-dependant epitopes. This may partly explain its broad spectrum of activity against aggregopathies. Well-defined structure-activity relationships (SARs) have provided insight on

1
2
3 the key structural features that determine its inhibitory potency.^{4, 9} The pyrazole ring, of all
4 heterocycles investigated, is most closely associated with the strong antiprion activity.
5 Molecular dynamics (MD) simulations suggest that the ring is effective at establishing
6 stabilising, transient, intermolecular hydrogen bonding interactions with the peptide backbone,
7 burying itself into the oligomeric structures.⁸ This binding mode is then strengthened by
8 hydrophobic contacts formed between the phenyl rings and the proteins' aromatic and aliphatic
9 side chains. Simulations suggest that the compound binds larger, ordered β -sheet filaments at
10 alternative sites however, burying into hydrophobic pockets at the expense of these hydrogen
11 bonding interactions.
12
13
14
15
16
17
18
19

20 Since the first reports on compound **1**, a number of research groups have produced powerful
21 *H*-bonding ligands effective at modulating protein aggregation. The heterocycles 2,6-
22 diaminopyridines and 3-substituted indoles, such as **2** and **3**, respectively (**Figure 1**), have been
23 identified as key binding motifs, when appropriately functionalised, and effective at inhibiting
24 the $A\beta_{1-42}$ aggregation *in vitro*.¹⁰⁻¹¹ Both **2** and **3** boast favourable BBB permeability in male
25 Swiss mice, though **2** exhibited poor metabolic stability, possibly accounting for its rapid
26 clearance. Mach and co-workers were able to tune the binding affinity of their novel scaffold
27 (**4**) for binding α -syn fibrils by altering the distance between hydrogen bonding groups. Their
28 SAR data suggested that hydrogen bonding may play a more important role in binding α -syn
29 than $A\beta$ or tau fibrils.¹²
30
31
32
33
34
35
36
37
38
39
40
41
42
43
44
45
46
47
48
49
50
51
52
53
54
55
56
57
58
59
60

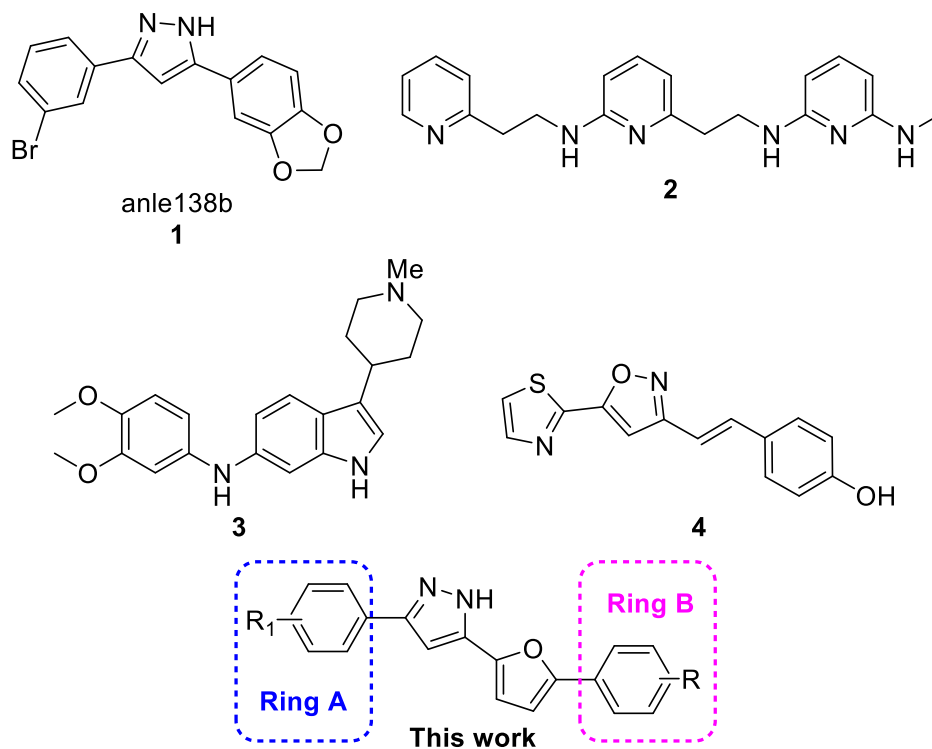


Figure 1. Structures of recently reported¹⁰⁻¹² inhibitors of amyloid formation and the generalised structure of the furan-2-yl-1*H*-pyrazoles investigated in this work.

Pyrazoles effectively form bidentate hydrogen bond contacts to amide hydrogens and carbonyl oxygens of the peptide backbones (**Figure 2**).¹³⁻¹⁴ It was speculated that the binding may improve as the number of *H*-bonding interactions increases accordingly. Aminopyrazole and related structures have been identified as potent ligands bearing high affinity for the top face of extending peptide strands.¹⁵ We were interested to probe how an increase in the number of potential hydrogen bond participating groups might affect the inhibitory activity of the analogues of anle138b. Consequently, it was decided to investigate a series of furan-2-yl-1*H*-pyrazoles bearing similar substitutions to the anle138b compound in the hope of improving biological activity. It was hypothesized that the furan oxygen may act as a hydrogen bond acceptor, without majorly altering the overall topological surface areas or lipophilicities of the resultant molecular structures. The furan ring was also chosen due to its relative structural simplicity, and its introduction would not increase the hydrogen bond donor count in the molecular structure. The hydrogen bond donor count represents a key CNS differentiating parameter.¹⁶ A recent analysis, from Eli Lilly, found the median HBD count for currently marketed CNS active drugs is 1, while the median HBA count is 4.¹⁶

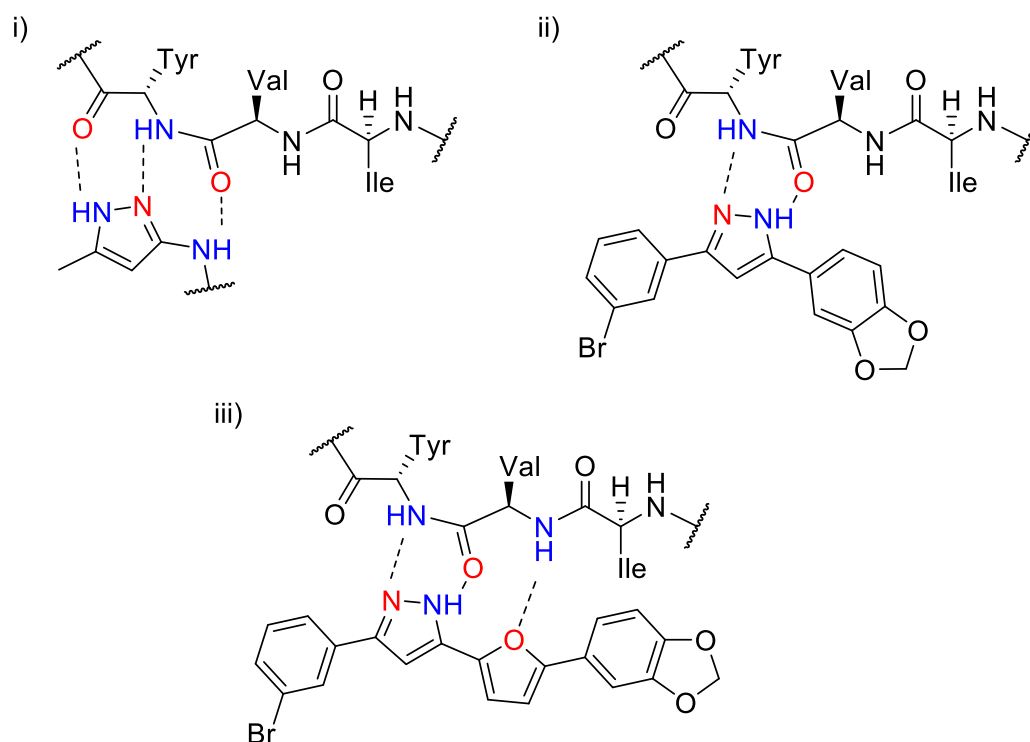


Figure 2. Binding scheme of a peptide backbone with i) methylaminopyrazole, ii) anle138b (**1**) and iii) a furan-2-yl-1*H*-pyrazole investigated here highlighting the differences in hydrogen-bond donor and acceptor properties.

For the current study, novel furan-2-yl-1*H*-pyrazoles and related chemical precursors were chosen for the activity against α -syn aggregation. The ThT fluorescence assays were employed to characterise the inhibitory activity and the MS-binding assay was used to probe the nature of the binding interaction with the protein.¹⁷ The results of inhibition studies led to the identification of a number of highly active pyrazole and pyrazoline derivatives more potent than the compound **1** *in vitro*. Molecular modelling studies were also conducted to examine the compounds' structural features and to evaluate binding energies. The human tau protein is a key protein involved in various proteopathic NDs. As with α -syn, tau exhibits a tendency to aggregate to form oligomers, which further leads to the generation of insoluble mass in the brain through aggregation. Although the exact mechanism of aggregation remains unknown it has been hypothesized that hydrogen bond formation in between peptides could play a major role. Furthermore, *in vitro* studies revealed that tau undergoes polymerization with the aid of an inducer conceivably α -syn *via* phosphorylation as reported by Gaisson et al.¹⁸ Hence, the molecular modelling analysis has been carried out using tau protein.

RESULTS AND DISCUSSION

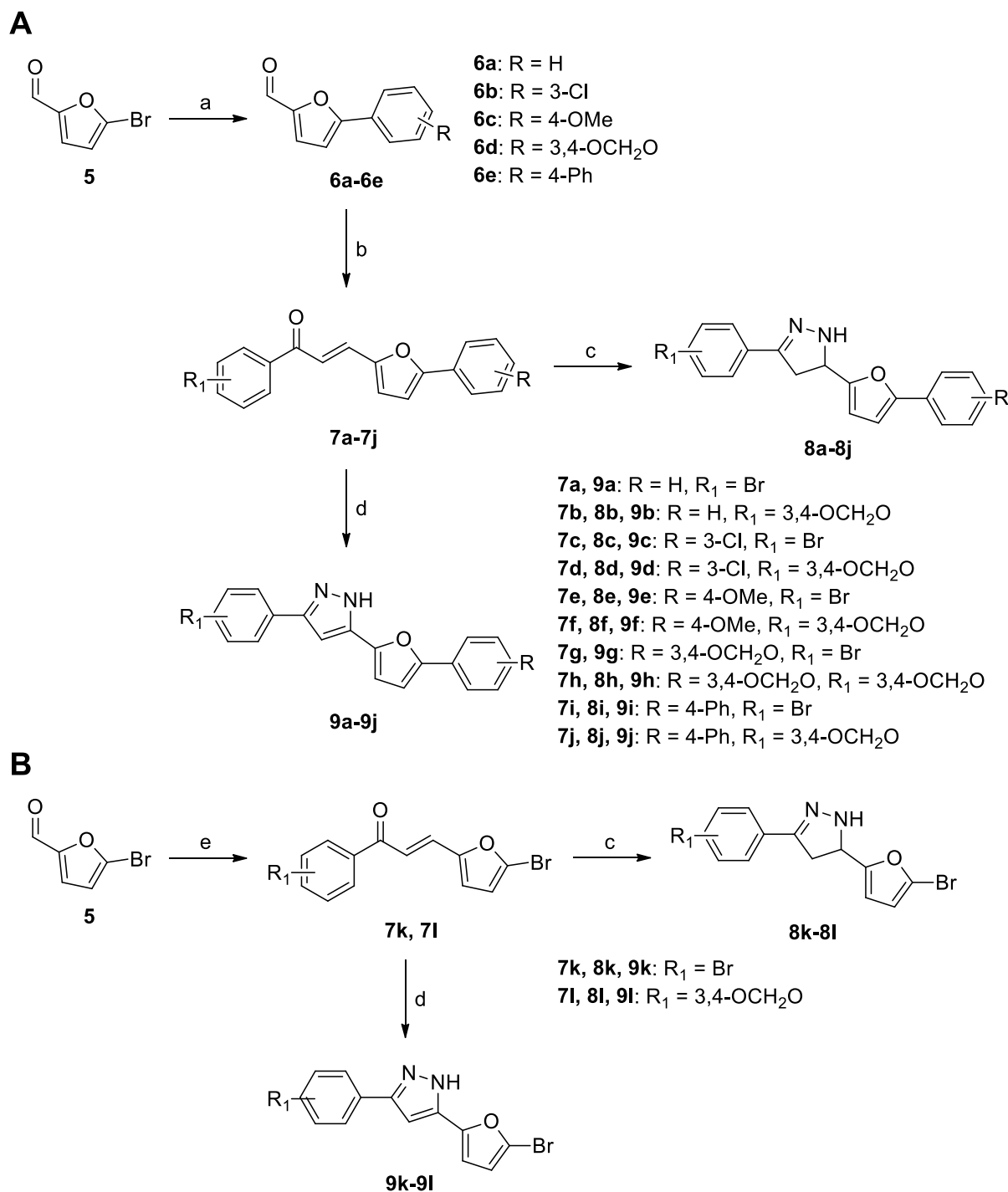
Chemistry

1
2
3
4
5
6
7
8
9
10
11
12
13
14
15
16
17
18
19
20
21
22
23
24
25
26
27
28
29
30
31
32
33
34
35
36
37
38
39
40
41
42
43
44
45
46
47
48
49
50
51
52
53
54
55
56
57
58
59
60

Previously, anle138b has been generated *via* the 1,3-diketo-intermediate.⁴ Considering rapid access to library of novel compounds, the synthesis of desired compounds was envisaged here *via* chalcone intermediates. Chalcones have displayed the inhibitory activity against α -syn aggregation,¹⁹ as well as high-affinity binding for the protein, and therefore, the synthetic precursors of the pyrazoles were evaluated also. Synthesis involved an initial Suzuki-Miyaura cross-coupling reaction of 5-bromo-2-furaldehyde **5** with various appropriately substituted phenylboronic acids before condensation with substituted acetophenone and subsequent generation of either the pyrazoline or pyrazole ring under microwave conditions (**Scheme 1**). The substitution on the phenyl rings strongly affects the bioavailability,⁴ therefore acetophenones and phenylboronic acids bearing the 1,3-benzodioxole or bulky halogens in the *meta*-position (compound **1**) were considered for conferring attractive physicochemical properties. The cross-coupling reactions of the furaldehydes forming **6a-6e** were typically high-yielding, however the reaction with 3-chlorophenylboronic acid afforded very poor yields of the desired product (**6b**). All attempts were made to improve the product yield by varying reaction conditions²⁰ (such as increasing temperature or molar equivalents of reactants of reactants and/or reagents) but failed. Interestingly, (*E*)-3-(5-(3-chlorophenyl)furan-2-yl)acrylaldehyde (SI, **Figure S1**), the product of ethanol's condensation with the 2-formyl derivatives was isolated as major product and the (*E*)-isomer was formed exclusively. To the best of our knowledge, this type of one-pot reaction has not been used previously to form this class of arylated furanoids.

Chalcones can be readily synthesized by the base-catalysed Claisen-Schmidt condensation of an aryl aldehyde and acetophenone derivative in a protic polar solvent like ethanol or methanol. The traditional chalcone synthesis involves the use of inorganic bases (NaOH, KOH, LiOH or Ba(OH)₂).²¹ Other protocols involve the use of organic bases also, such as piperidine.²² Employing aldol condensation to form chalcones (**7a-7j**) was initially attempted following by established protocols, specifically using NaOH in EtOH at room temperature overnight.²³⁻²⁴ The diarylated chalcone synthesis worked well (data not included). However, synthesis using heteroaryl aldehydes (eg. 2-furaldehyde) frequently resulted in poor reaction yields due to the formation of complex mixtures of side-products which were challenging to isolate. When conducted under microwave-assisted heating conditions however, the reactions afforded the desired product quantitatively. Additionally, the reaction time was dramatically improved, being reduced from upward of 5 h to only 30 min. With chalcones in hand, pyrazoles (**9a-9j**) were generated using hydrazine hydrate with sulfur as an oxidant under microwave-

1
2
3 assisted heating conditions.²⁵ Though the reaction yields were not exceptional, they produced
4 an acceptable amount of desired compounds for the biological evaluation. The poor yields
5 suggested that sulfur may not have been an effective oxidizing agent, as the reactions yielding
6 pyrazolines (**8b-8j**) were characterized by significantly increased yields. The synthesis of 5-
7 bromofuran-2-yl pyrazoles **9k** and **9l** were also attempted but isolation could not be carried out
8 due to decomposition into the unsubstituted furfural derivatives, which were confirmed by
9 NMR and MS.
10
11
12
13
14
15
16
17
18
19
20
21
22
23
24
25
26
27
28
29
30
31
32
33
34
35
36
37
38
39
40
41
42
43
44
45
46
47
48
49
50
51
52
53
54
55
56
57
58
59
60



Scheme 1. Synthesis of chalcone, pyrazoline and pyrazole analogues **7a-9j** (A) and **7k-9l** (B). *Reagents and conditions:* (a) ArB(OH)₂, Pd(PPh₃)₄, PhMe, EtOH, K₂CO₃(aq), reflux, 16 h; 40-98%; (b) acetophenone (1 eq.), EtOH, piperidine, MW, 70 °C, 30 min, 80-97%; (c), NH₂NH₂, EtOH, MW, 70 °C, 1 h, 59-87%; (d); NH₂NH₂, EtOH, S, MW, 150 °C, 2 h, 13-42%; (e) acetophenone (1 eq.), EtOH, NaOH, rt, 16 h, 81-97%.

Biology

The ability of the compounds to inhibit α -syn aggregation was studied by incubating α -syn (80 μ M), expressed in *E.coli* and purified using anion exchange, with or without the compounds (400 μ M) under constant agitation for 48 hours before being analysed by ThT fluorescence. It was decided to see the effect of the compounds at the end-point of the experiment, rather than any effects on the rate of aggregation, as ThT has been found previously to alter aggregation kinetics.²⁶ Two positive controls were examined, synthetically produced anle138b and commercially available EGCG, with six replicates per sample being used.

Treatment with chalcones **7a-7l** reduced fluorescence by values ranging from 58% (**7c**) to 80% (**7e**) (**Figure 3**). It was noted that the substitution of ring A with 3-Br often yielded compounds more effective at reducing fluorescence than those substituted with the 1,3-benzodioxole. It was also noted that substitution of ring B with 4-methoxy or 1,3-benzodioxole groups yielded more effective compounds as compared to those bearing larger groups such as 3-Cl or 4-phenyl. Chalcones **7k** and **7l**, generated *via* aldol condensation with unmodified 5-bromo-2-furaldehyde, were also evaluated. Fluorescence values were decreased five-fold following treatment with **7k**, compared to 1,3-benzodioxole-substituted **7l**. Of all the chalcones evaluated, only **7e** and **7k** displayed effects comparable to anle138b.

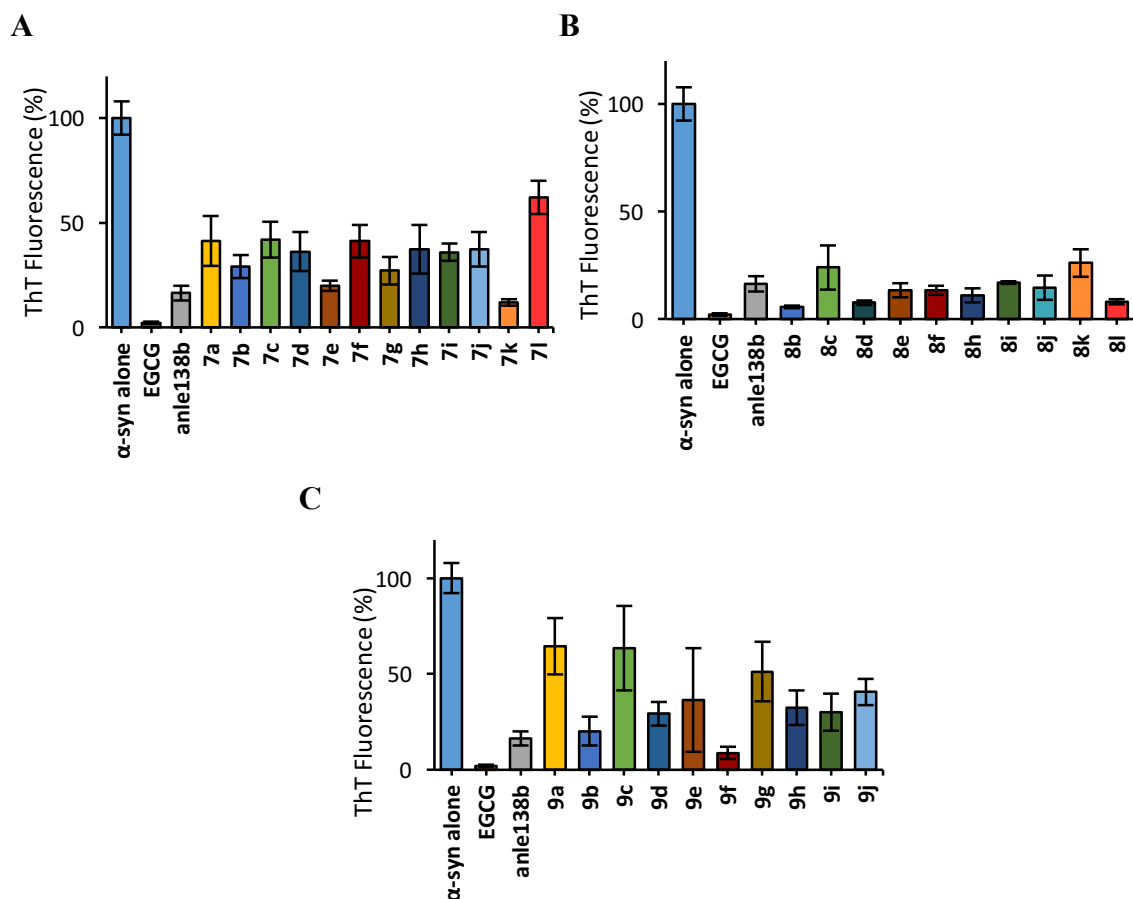


Figure 3. Aggregation of α -syn was measured by ThT fluorescence assay. Chalcones' (A), pyrazolines' (B), and pyrazoles' (C) effects on fluorescence were examined using a 1:5 α -syn to compound molar ratio (80:400 μ M). The data are expressed as mean of six independent experiments. Data are expressed as percentage (mean \pm standard deviation) of untreated negative control (α -syn only) and compared to positive control treated with epigallocatechin gallate (EGCG) and anle138b. Colours correlate with ring substitution patterns common between the compound panels.

Pyrazolines **8b-8l** reduced fluorescence by values in the range of 76% (**8c**) to 94% (**8b**) (**Figure 3B**). In the case of the pyrazolines, more often than not substitution with 1,3-benzodioxole on ring A was associated with a larger decrease in fluorescence than 3-Br substitution. Interestingly, these results contrast with the trends observed for the chalcones. Again, smaller substitutions on ring B tended to reduce fluorescence more significantly. Pyrazolines **8k** and **8l**, arising from the reaction of hydrazine with chalcones **7k** and **7l** respectively, were also tested. The 1,3-benzodioxole-substituted **8l** decreased fluorescence by four-fold relative to **8k**. Under the assay conditions here, the majority of pyrazolines were as effective as anle138b at reducing levels of fluorescence. Notably three of the pyrazolines, **8b** ($p < 0.01$), **8d** ($p < 0.05$), and **8l** ($p < 0.05$), decreased fluorescence more significantly than the anle138b compound.

The pyrazoles **9a-9j** displayed inhibition of α -syn aggregation in the range of 36% (**9a**) to 91% (**9f**) (**Figure 3C**). Among the pyrazoles examined, the most effective inhibitor was **9f**, the compound bearing 1,3-benzodioxole substitution on ring A and 4-methoxy substitution on ring B. It was observed that 1,3-benzodioxole substitutions on ring A typically resulted in stronger reducers of fluorescence than the 3-Br substitution, as observed in the case of the pyrazolines. Again, smaller substitutions on ring B yielded more effective compounds also. Attempts to generate pyrazoles brominated at the C-5 position on the furan ring were unsuccessful as the desired products were subject to rapid degradation. Under the assay conditions here, a majority of the pyrazoles were less effective than the anle138b compound at reducing levels of ThT fluorescence with the exception of compounds **9b** and **9f** which displayed similar potencies.

Of all the compounds examined, the most significant decreases in ThT fluorescence resulted from co-incubation of α -syn with pyrazolines **7k**, **8b**, **8d** and **8l** and with pyrazole **9f**. The most interesting compounds **8b**, **8l** and **9f** were chosen and tested at two different molar ratios to examine whether the decreases in fluorescence may be dose-dependent. Interestingly, although the pyrazole **9f** at a 1:5 molar ratio decreased fluorescence by an amount comparable to anle138b, at stoichiometric concentration it was less effective, seemingly even promoting fluorescence. Pyrazolines **8b** and **8l** seemed to reduce fluorescence at both concentrations tested. Interestingly, **8b** decreased fluorescence to a similar degree under both concentrations tested.

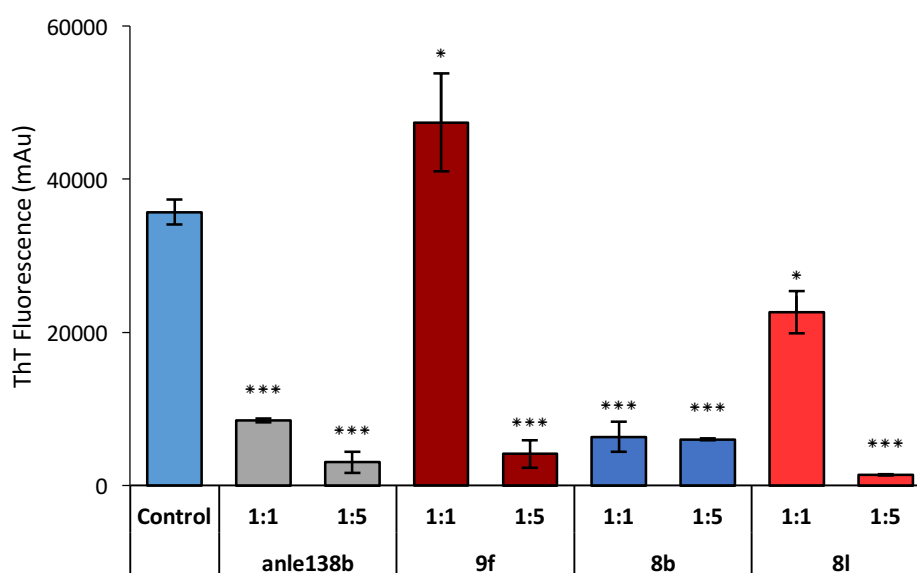


Figure 4. Inhibition of aggregation measured by ThT fluorescence assay at 1:5 and 1:1 molar ratio α -syn/compound. The data are expressed as mean of 3 independent experiments. Data are expressed as percentage (mean \pm standard deviation) of untreated negative control (α -syn only) and compared to positive control treated with anle138b. Data was analysed using one-way ANOVA with Dunnett's post hoc comparison (* p <0.05 vs control; *** p <0.001 vs control).

The inhibition of fibril formation was validated using dot blot analysis, a non-denaturing method for examining protein epitopes. Dot blot analysis has been employed previously to study α -syn fibril formation and inhibitor-bound α -syn complexes structural conformations.²⁷⁻²⁸ Equal volumes of each sample (2 μ L) were spotted on nitrocellulose membrane before being stained with one of either the non-conformation dependent anti- α -syn antibody (1:2,000) or the conformation dependent anti- α -syn filament antibody (1:8,000) prior to further staining with a detection antibody.²⁹⁻³⁰ Development of the blots exhibited notable signal intensity of fibrillary and total α -syn, which was analysed for quantification (**Figure 5**). All compounds were found to decrease concentration of fibrillar α -syn at both molar equivalents tested (1:1, 1:5, α -syn/compound) relative to the untreated control. Dose-dependent effects were observed for anle138b and compounds **8b** and **8l**, with compound **8b** decreasing the concentration of fibrillar α -syn detected most effectively. Interestingly, dose-dependent effects on fibril concentration were not displayed for compound **9f**, which had worked previously to increase fluorescence at 1:1 molar ratio in the ThT assay. Rather compound **9f** reduced the concentration of fibrillar α -syn detected by ~80 % consistently in this case.

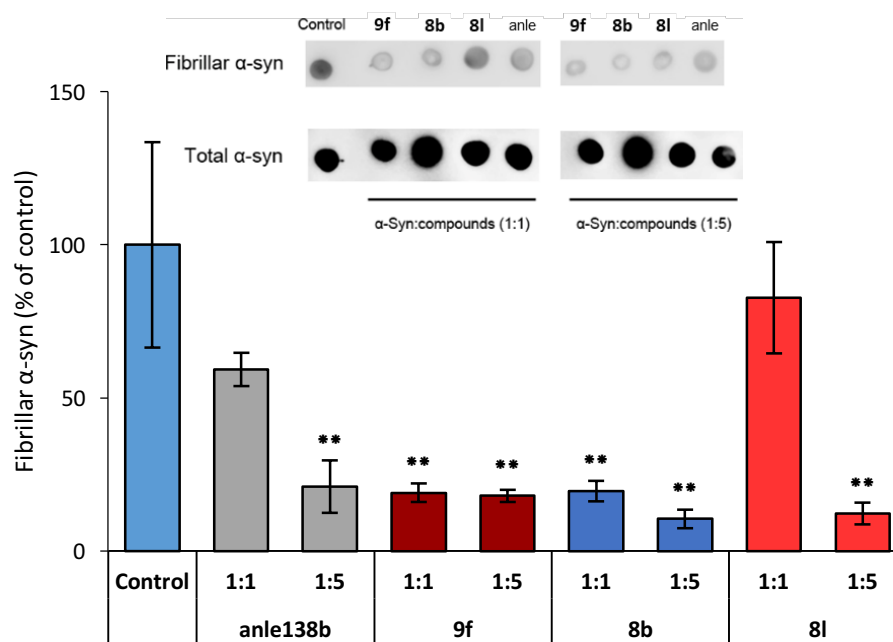


Figure 5. Dot blot analysis of α -syn fibril formation relative to an untreated control. Presence of α -syn in each sample was confirmed *via* staining with anti- α -synuclein antibody. In samples treated with conformation dependent anti- α -synuclein filament antibody, the total α -syn dot blot quantification was used to normalize the fibrillary α -syn staining. Data are expressed as percentage (mean \pm standard deviation) of untreated negative control (α -syn only, taken as 100, n = 3) and compared to positive control treated with anle138b (**1**). Data was analysed using one-way ANOVA with Dunnett's post hoc comparison (** p<0.01 vs control).

1
2
3
4
5
6
7
8
9
10
11
12
13
14
15
16
17
18
19
20
It is interesting to note that in most of the cases the pyrazoline derivatives were found to be more effective at reducing ThT fluorescence than their structural analogues (pyrazole derivatives) possessing equivalent substitution patterns. To rationalize the observed trend in the biological results, molecular docking analysis has been carried out. The binding affinity has been estimated in terms of Glide scores,³¹⁻³² Induced Fit Docking³³⁻³⁴ (IFD) scores (data listed in **Table S1**). The binding energies associated with docked (1st ranked) poses have been estimated using Prime MMGBSA tool.³⁵ **Figure 6** shows two views of binding pocket chosen to perform molecular docking. The identified binding cavity has a C_2 symmetric elliptical cone shape with hydrophobic component in the centre of the cavity (yellow color, **Figure 6: A and B**).

21
22
23
24
25
26
27
28
29
30
31
32
33
34
35
36
37
38
39
40
41
42
43
44
45
46
47
48
49
50
The mechanism of aggregation of oligomers involves interpeptide main chain interaction due to the formation of hydrogen bonds. Anle138b effectively inhibits the interpeptide main chain interaction, by occupying the C_2 symmetric elliptical cavity (especially the hydrophobic pocket of the macromolecule, the dimer of β -sheet). The important amino acids responsible for this binding are ILE4, VAL5, PHE10 and TYR6 amino acid residues (from each monomer). The two nitrogen atoms of the pyrazole ring face away from the centre of the cavity and form hydrogen bonds with the back bone atoms of the peptide chains (the dimer of β -sheet near to the proximity of ILE4 of C and D chain). This interaction is responsible for the inhibition of the interpeptide hydrogen bond formation and thus for the inhibition of the aggregation. The hydrophobic residues of cavity i.e. TYR6 of D chain & PHE10 of C and D chains of dimer of β -sheet comes in contact with phenyl rings of molecules *via* π - π stacking into the hydrophobic pocket in the docked pose. The lead compound anle138b exhibits very strong binding affinity -- the Glide score -6.84, IFD score -54.30 and the Prime MMGBSA binding energy value -949.20 kcal/mol (**Table S1**). This strong binding affinity is originating from the specific interaction involving two hydrogen bonds between pyrazole moiety of compound anle138b with central aliphatic ILE4 of C & D chain and hydrophobic interactions between phenyl ring of compound with the Phe10 of C and D chains of the β -sheet.

51
52
53
54
55
56
57
58
59
60
Compound **8b** exhibits better binding affinity in comparison to the lead compound because of the additional hydrogen bond interaction in the pyrazoline moiety (i.e. TYR D: 6 in interpeptide backbone; **Figure 7: A and B**). Molecular docking analysis was performed using both the *R* and *S* isomers of the considered compounds. However, the *S* isomer was considered in further studies because it showed better binding affinity on a comparative scale. Further, 11 compounds (**7c**, **7h**, **8c**, **8d**, **8e**, **8f**, **9c**, **9d**, **9f**, **9g** and **9h**) can be considered as competitors to

the lead compound. Two compounds **8h** and **8l** are worth considering for further modification because these are in the border line. This conclusion is based on the cut off values Glide score > -6.0 , IFD score > -40 and Prime MMGBSA > -800 kcal/mol. The pyrazoline core is considerably more capable at engaging with the C_2 symmetric cavity, due to the scaffolds increased flexibility, which may explain the ability of the pyrazolines to reduce ThT fluorescence more significantly than the other compounds.

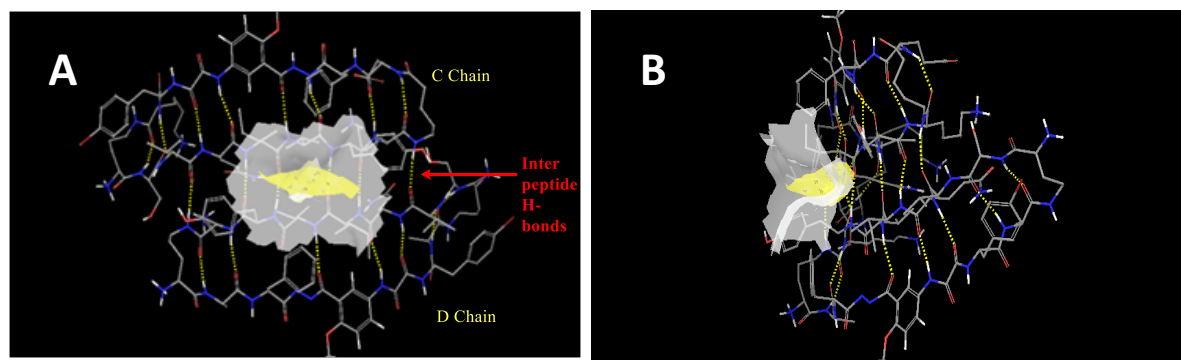


Figure 6. Identification of the hydrophobic active site of the β -sheets of hTau protein in which the Anle138b and synthesized compounds bind. (A) Front view and (B) side view of hydrophobic binding site. Yellow color component in centre represents hydrophobic active site in between two β -sheet.

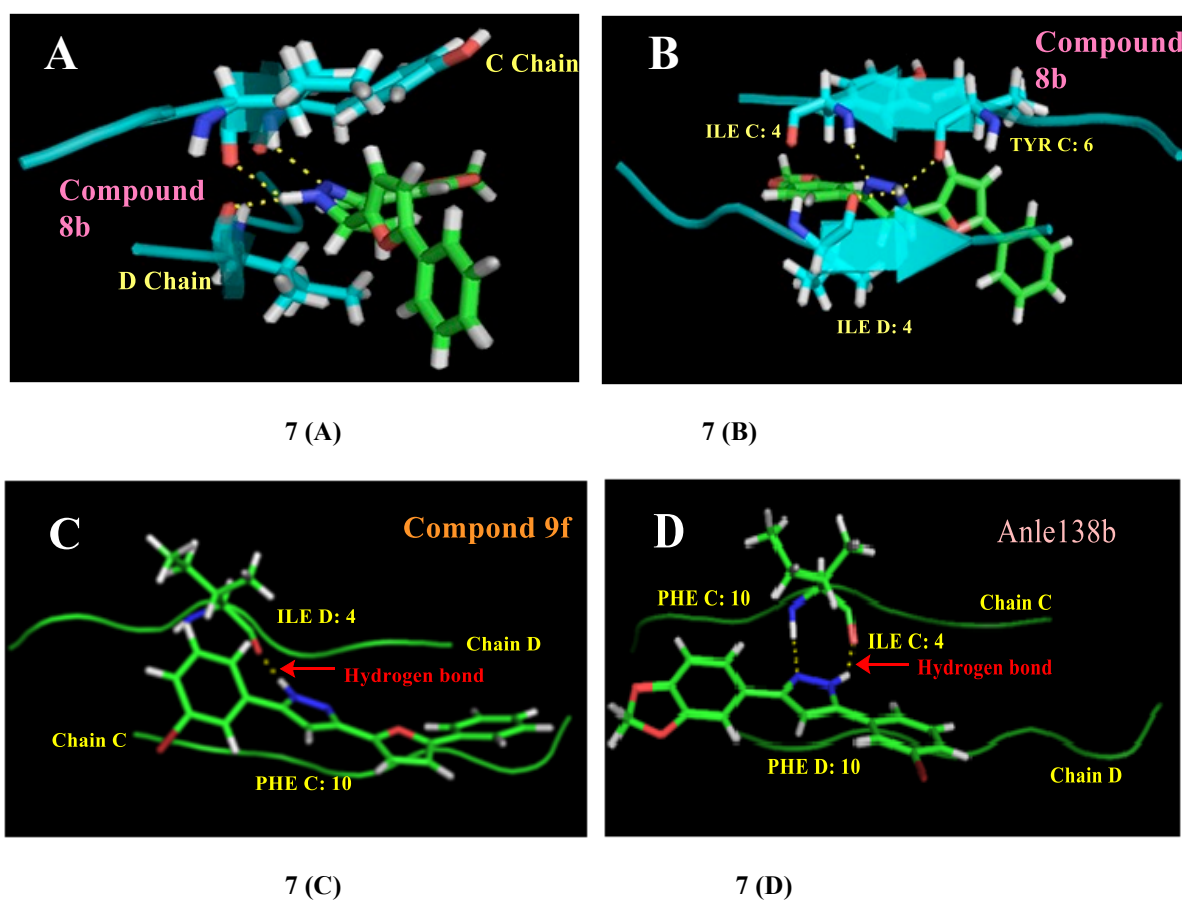


Figure 7. Interactions between **8b** and the active site residues of dimer of β -sheet where the interpeptide hydrogen bonds are formed in between the ILE and TYR residues of backbone peptide chain with the pyrazoline nitrogens therefore, inhibit the interpeptide hydrogen bond formation. (7A) Front view, (7B) side view. **9f** compound representative of synthesized pyrazole class which interacts with active hydrophobic side *via* the formation of hydrogen bond with ILE D: 4 showed in Figure 7(C). Interaction of Anle138b with the binding site involves formation of the two hydrogen bonds and showed hydrophobic interaction with PHE 10 (7 D).

The ADME profile of the synthesized compounds was estimated using SWISS ADME profile online server. The results are listed in **Table S2** (ESI). Almost all the synthesized compounds exhibited good bioavailability properties, satisfy the Lipinski's rule of five. Most of them are also CNS permeable as per the computational estimation.

The chemical properties of these species were evaluated using Chem3D Ultra 15.1 (using ChemPropStd module and the molecular topology property module; **Table S3**). Clearly, the chemical properties of **8b** are larger in terms of topological diameter, accessible surface area, polar surface area and the shape attribute in comparison to that of the lead compound anle138b.

In summary, novel pyrazoles analogues were identified which are capable of significantly inhibiting the aggregation of α -syn characteristically seen in PD pathology. A number of the compounds were found to possess inhibitory activity in the range of the preclinical drug anle138b. Compound **9f** was identified as a lead pyrazole while compounds **8b** and **8l** were identified as lead pyrazolines species towards the inhibition of α -syn aggregation. Molecular modelling studies employing molecular docking and including induce fit effect provided clues regarding the inhibitory effect exhibited by the new leads suggested above. In comparison with anle138b, one or more of these novel compounds may serve as secondary leads for further SAR studies and development of anle138b analogues possessing desirable physicochemical properties.

METHODS

General Methods. Proton nuclear magnetic resonance (^1H NMR) spectra were recorded using a Bruker AVANCE DPX 400 spectrometer at a frequency of 400.2 MHz. Carbon nuclear magnetic resonance (^{13}C NMR) spectra were recorded on a Bruker Avance DPX 400 spectrometer at a frequency of 100 MHz. The spectra are reported as parts per million (ppm) downfield shift using the solvent peak as internal reference. The data are reported as chemical shift (δ), multiplicity, relative integral, coupling constant (J , Hz) and assignment where possible. For pyrazole-containing compounds **9a-9j**, one drop of trifluoroacetic acid was added to the NMR solvent to stabilise tautomerism and simplify interpretation. Low resolution mass spectra were recorded on a Finnigan LCQ Deca ion trap spectrometer (ESI). High resolution

mass spectra were recorded on a Bruker 7T Fourier Transform Ion Cyclotron Resonance Mass Spectrometer (FTICR). Analytical thin layer chromatography (TLC) was performed using commercially prepared silica plates (Merck Kieselgel 60 0.25 mm F254). Flash column chromatography was performed using 230-400 mesh Kieselgel 60 silica eluting with analytical grade solvents. Reagents, catalysts and solvents were purchased from Sigma-Aldrich, AK Scientific and Chem-Supply and were used as received unless otherwise noted.

General Procedure for Preparations of Compounds 6a-6e. To a stirred suspension of 5-bromo-2-furaldehyde (0.50 g, 2.9 mmol) in toluene/ethanol/aq. potassium carbonate (2:1:2 v/v/v 25 mL) was added phenylboronic acid (1.1 equiv., 3.1 mmol). The reaction vessel was then charged with [tetrakis(triphenylphosphine)]palladium(0) complex (0.01 equiv., 0.032 g, 0.029 mmol) before heating to reflux. The mixture was left stirring for 16 h before being allowed to cool to room temperature and diluted with ethyl acetate (30 mL), washed with water (10 mL), brine and then dried over Na₂SO₄. The solution was then filtered and concentrated under reduced pressure before being purified by flash chromatography (EtOAc/hexane 1:1) to give aryl substituted furaldehydes.

5-phenylfuran-2-carbaldehyde (6a): Yellow oil, 93% yield, ¹H NMR (500 MHz CDCl₃): δ 9.65 (s, 1H, CHO), 7.84-7.81 (m, 2H, ArH), 7.47-7.38 (m, 3H, ArH), 7.32 (d, *J* = 3.6 Hz, 1H, furan CH), 6.84 (d, *J* = 3.6 Hz, 1H, furan CH); ¹³C NMR (126 MHz CDCl₃): δ 177.3, 159.5, 152.1, 129.7, 129.0 (3 x C), 125.3 (2 x C), 123.6 (broad), 107.7.

5-(3-chlorophenyl)furan-2-carbaldehyde (6b): Orange flake, 40% yield, ¹H NMR (400 MHz CDCl₃): δ 9.67 (s, 1H, CHO), 7.80 (dd, *J* = 1.4, 0.6 Hz, 1H, ArH), 7.69 (ddd, *J* = 1.8, 2.4, 6.4 Hz, 1H, ArH), 7.39-7.36 (m, 2H, 2 x ArH), 7.32 (d, *J* = 3.8 Hz, 1H, furan CH), 6.86 (d, *J* = 3.7 Hz, 1H, furan CH). ¹³C NMR (101 MHz CDCl₃): δ 177.4, 157.7, 152.3, 135.1, 130.6, 130.3, 129.6, 125.3, 123.3, 100.5.

5-(4-methoxyphenyl)furan-2-carbaldehyde (6c): Red flake, 98% yield, ¹H NMR (400 MHz CDCl₃): δ 9.60 (s, 1H, CHO), 7.76 (d, *J* = 8.9 Hz, 2H, 2 x ArH), 7.30 (d, *J* = 3.7 Hz, 1H, furan CH), 6.97 (d, *J* = 8.9 Hz, 2H, 2 x ArH), 6.71 (d, *J* = 3.7 Hz, 1H, furan CH), 3.86 (s, 3H, CH₃); ¹³C NMR (101 MHz CDCl₃): δ 176.9, 160.9, 159.8, 151.6, 127.0 (2 x C), 121.8, 114.8, 114.4 (2 x C), 106.3, 55.4.

5-(benzo[*d*][1,3]dioxol-5-yl)furan-2-carbaldehyde (6d): Yellow-orange flake, 92% yield. ¹H NMR (400 MHz CDCl₃): δ 9.60 (s, 1H, CHO), 7.36 (dd, *J* = 8.2, 1.7 Hz, ArH), 7.90 (d, *J* = 3.8 Hz, 1H, furan CH), 7.27 (d, *J* = 1.7 Hz, 1H, ArH), 6.87 (d, *J* = 8.2 Hz, 1H, ArH), 6.69 (d,

1
2
3
4
5
6
7
8
9
10
11
12
13
14
15
16
17
18
19
20
21
22
23
24
25
26
27
28
29
30
31
32
33
34
35
36
37
38
39
40
41
42
43
44
45
46
47
48
49
50
51
52
53
54
55
56
57
58
59
60

$J = 3.7$ Hz, 1H, furan *CH*), 6.02 (s, 2H, CH_2); ^{13}C NMR (101 MHz CDCl_3): δ 176.9, 159.4, 151.4, 149.1, 148.3, 123.9, 123.2, 120.1, 108.9, 106.7, 105.6, 101.6.

5-([1,1'-biphenyl]-4-yl)furan-2-carbaldehyde (6e): Orange solid, 62% yield, ^1H NMR (400 MHz CDCl_3): δ 9.67 (s, 1H, *CHO*), 7.91 (d, $J = 8.6$ Hz, 2H, *ArH*), 7.69 (d, $J = 8.6$ Hz, 2H, *ArH*), 7.64 (d, $J = 7.2$ Hz, 2H, *ArH*), 7.47 (t, $J = 7.2$ Hz, 2H, *ArH*), 7.39 (t, $J = 7.2$ Hz, 1H, *ArH*), 7.34 (d, $J = 3.7$ Hz, 1H, furan *CH*), 6.88 (d, $J = 3.7$ Hz, 1H, furan *CH*); ^{13}C NMR (101 MHz CDCl_3): δ 177.2, 159.3, 152.1, 142.4, 140.1, 128.9 (2 x C), 127.9 (2 x C), 127.6 (2 x C), 127.0 (2 x C), 125.8 (2 x C), 123.6 (broad), 107.8.

General Procedure for Preparations of Compounds 7a-7j. To a stirred suspension of 5-aryl-2-furaldehyde (0.2 g) in ethanol (2.0 mL) was added substituted acetophenone (1.1 equiv.) and piperidine (0.03 mL, 0.03 mmol). The reaction vessel was purged with argon and then heated with microwave irradiation (300 W of max. power) to 70 °C. The pressure limit was set to 190 *psi*. Once the desired temperature was reached over 5 minutes, heating was continued for a further 20 min to maintain temperature. The mixture was then allowed to cool to room temperature before being concentrated under reduced pressure. The mixture was then resuspended in ethanol/water (1:1 v/v), isolated using filtration and recrystallised from ethanol to give highly pure chalcones.

(E)-1-(3-bromophenyl)-3-(5-phenylfuran-2-yl)prop-2-en-1-one (7a): Yellow solid, 93% yield, ^1H NMR (400 MHz CDCl_3): δ 8.18 (t, $J = 1.8$ Hz, 1H, *ArH*), 7.97 (dt, $J = 1.2, 7.8$ Hz, 1H, *ArH*), 7.80-7.79 (m, 2H, *ArH*), (ddd, $J = 0.9, 1.8, 7.8$ Hz, 1H, *ArH*), 7.63 (d, $J = 15.2$ Hz, 1H, *CH*), 7.47-7.34 (m, 4H, *ArH*), 7.42 (d, $J = 15.2$ Hz, 1H, *CH*), 6.85 (d, $J = 3.6$ Hz, 1H, furan *CH*), 6.80 (d, $J = 3.6$ Hz, 1H, furan *CH*); ^{13}C NMR (101 MHz CDCl_3): δ 188.4, 156.8, 151.0, 140.2, 135.5, 131.4, 131.2, 130.2, 129.7, 128.9, 128.8, 126.9, 124.6, 123.0, 119.6, 117.9, 108.4.

(E)-1-(benzo[*d*][1,3]dioxol-5-yl)-3-(5-phenylfuran-2-yl)prop-2-en-1-one (7b): Orange solid, 88% yield, ^1H NMR (400 MHz CDCl_3): δ 7.79-7.77 (m, 2H, *ArH*), 7.70 (dd, $J = 8.2, 1.7$ Hz, 1H, *ArH*), 7.60 (d, $J = 15.2$ Hz, 1H, *CH*), 7.57 (d, $J = 1.7$ Hz, 1H, *ArH*), 7.47 (d, $J = 15.2$ Hz, 1H, *CH*), 7.46-7.42 (m, 2H, *ArH*), 7.36-7.33 (m, 1H, *ArH*), 6.92 (d, $J = 8.2$ Hz, 1H, *ArH*), 6.80 (d, $J = 3.6$ Hz, 1H, furan *CH*), 6.78 (d, $J = 3.6$ Hz, 1H, furan *CH*), 6.07 (s, 2H, CH_2); ^{13}C NMR (101 MHz CDCl_3): δ 187.6, 156.3, 151.6, 151.2, 148.3, 133.2, 130.1, 129.9, 128.9 (2 x C), 128.6, 124.6, 124.5 (2 x C), 118.6, 118.4, 108.4, 108.2, 108.0, 101.9; HRMS (ESI) 319.0959 ($[\text{M} + \text{H}]^+$), calcd. for $\text{C}_{20}\text{H}_{15}\text{O}_4^+$ 319.0965.

(E)-1-(3-bromophenyl)-3-(5-(3-chlorophenyl)furan-2-yl)prop-2-en-1-one (7c): Yellow solid. 80% yield, ^1H NMR (400 MHz CDCl_3): δ 8.18 (t, $J = 1.7$ Hz, 1H, *ArH*), 7.98 (dt, $J = 7.8, 1.3$ Hz, 1H, *ArH*), 7.76 (t, $J = 1.7$ Hz, 1H, *ArH*), 7.72 (ddd, $J = 0.9, 1.9, 7.9$ Hz, 1H, *ArH*),

7.66 (dt, $J = 7.7, 1.4$ Hz, 1H, ArH), 7.62 (d, $J = 15.2$ Hz, 1H, CH), 7.44 (d, $J = 15.2$ Hz, 1H, CH), 7.41 (t, $J = 7.9$ Hz, 1H, ArH), 7.38 (t, $J = 7.86$ Hz, 1H, ArH), 7.32 (ddd, $J = 1.2, 1.9, 8.0$ Hz, 1H, ArH), 6.85 (d, $J = 3.6$ Hz, 1H, furan CH), 6.82 (d, $J = 3.6$ Hz, 1H, furan CH); ^{13}C NMR (101 MHz CDCl_3): δ 188.3 155.1, 151.4, 140.0, 135.6, 135.0, 131.4 (2 x C), 131.0, 130.2 (2 x C), 128.6, 127.0, 124.5, 123.0, 122.6, 119.3, 118.6, 109.3.

(E)-1-(benzo[d][1,3]dioxol-5-yl)-3-(5-(3-chlorophenyl)furan-2-yl)prop-2-en-1-one

(7d): Fluorescent yellow solid, 86% yield, ^1H NMR (400 MHz CDCl_3): δ 7.75 (t, $J = 1.7$ Hz, 1H, ArH), 7.70 (dd, $J = 8.2, 1.7$ Hz, 1H, ArH), 7.64 (dt, $J = 7.7, 1.3$ Hz, 1H, ArH), 7.58 (d, $J = 15.2$ Hz, 1H, CH), 7.56 (d, $J = 1.7$ Hz, 1H, ArH), 7.47 (d, $J = 15.2$ Hz, 1H, CH), 7.37 (t, $J = 7.8$ Hz, 1H, ArH), 7.30 (ddd, $J = 1.3, 1.7, 8.0$ Hz, 1H, ArH), 6.93 (d, $J = 8.2$ Hz, 1H, ArH), 6.80 (d, $J = 3.8$ Hz, 1H, furan CH), 6.79 (d, $J = 3.8$ Hz, 1H, furan CH), 6.07 (s, 2H, CH_2); ^{13}C NMR (101 MHz CDCl_3): δ 187.6, 154.6, 151.7 (2 x C), 148.3, 135.0, 133.0, 131.5, 130.1, 129.9, 128.4, 124.7, 124.4, 122.5, 119.0, 118.4, 109.1, 108.4, 108.0, 101.9; HRMS (ESI) 353.0558 ($[\text{M} + \text{H}]^+$), calcd. for $\text{C}_{20}\text{H}_{14}\text{ClO}_4^+$ 353.0575.

(E)-1-(3-bromophenyl)-3-(5-(4-methoxyphenyl)furan-2-yl)prop-2-en-1-one (7e):

Yellow solid, 95% yield, ^1H NMR (400 MHz CDCl_3): δ 8.17 (t, $J = 1.7$ Hz, 1H, ArH), 7.97 (dt, $J = 1.3, 6.6$ Hz, 1H, ArH), 7.73 (d, $J = 8.9$ Hz, 2H, 2 x ArH), 7.70 (ddd, $J = 0.9, 1.9, 7.9$ Hz, 1H, ArH), 7.61 (d, $J = 15.1$ Hz, 1H, CH), 7.39 (t, $J = 7.9$ Hz, 1H, ArH), 7.39 (d, $J = 15.1$ Hz, 1H, CH), 6.98 (d, $J = 8.9$ Hz, 2H, 2 x ArH), 6.83 (d, $J = 3.6$ Hz, 1H, furan CH), 6.67 (d, $J = 3.6$ Hz, 1H, furan CH), 3.87 (s, 3H, CH_3); ^{13}C NMR (101 MHz CDCl_3): δ 188.4, 160.2, 157.1, 150.4, 140.3, 135.4, 131.4, 131.3, 130.2, 126.9, 126.2 (2 x C), 122.9, 122.7, 120.0, 117.2, 114.4 (2 x C), 107.0, 55.4.

(E)-1-(benzo[d][1,3]dioxol-5-yl)-3-(5-(4-methoxyphenyl)furan-2-yl)prop-2-en-1-one

(7f): Orange solid, 93% yield, ^1H NMR (400 MHz CDCl_3): δ 7.72 (d, $J = 8.9$ Hz, 2H, 2 x ArH); 7.69 (dd, $J = 1.8, 8.1$ Hz, 1H, ArH), 7.58 (d, $J = 15.3$ Hz, 1H, CH), 7.56 (d, $J = 2.0$ Hz, 1H, ArH), 7.43 (d, $J = 15.3$ Hz, 1H, CH), 6.97 (d, $J = 8.9$ Hz, 2H, 2 x ArH), 6.91 (d, $J = 8.0$ Hz, 1H, ArH), 6.78 (d, $J = 3.6$ Hz, 1H, furan CH), 6.65 (d, $J = 3.6$ Hz, 1H, furan CH), 6.07 (s, 2H, CH_2), 3.87 (s, 3H, CH_3); ^{13}C NMR (101 MHz CDCl_3): δ 187.7, 160.0, 156.6, 151.6, 150.7, 148.3, 133.3, 130.2, 126.1, 124.5, 122.9, 119.0, 117.7, 114.3, 108.4, 107.9, 106.8, 101.8, 55.4; HRMS (ESI) 349.1070 ($[\text{M} + \text{H}]^+$), calcd. for $\text{C}_{21}\text{H}_{17}\text{O}_5^+$ 349.1071.

(E)-3-(5-(benzo[d][1,3]dioxol-5-yl)furan-2-yl)-1-(3-bromophenyl)prop-2-en-1-one

(7g): Yellow solid, 90% yield, ^1H NMR (400 MHz CDCl_3): δ 8.16 (t, $J = 1.7$ Hz, 1H, ArH), 7.96 (d, $J = 7.8$, 1H, ArH), 7.70 (ddd, $J = 0.9, 1.9, 8.0$ Hz, 1H, ArH), 7.60 (d, $J = 15.2$ Hz, 1H,

1
2
3
4
5
6
7
8
9
10
11
12
13
14
15
16
17
18
19
20
21
22
23
24
25
26
27
28
29
30
31
32
33
34
35
36
37
38
39
40
41
42
43
44
45
46
47
48
49
50
51
52
53
54
55
56
57
58
59
60

CH), 7.39 (t, $J = 7.5$ Hz, 1H, *ArH*), 7.37 (d, $J = 15.2$ Hz, 1H, *CH*), 7.32 (dd, $J = 8.1, 1.7$ Hz, 1H, *ArH*), 7.24 (d, $J = 1.6$ Hz, 1H, *ArH*), 6.89 (d, $J = 8.2$ Hz, 1H, *ArH*), 6.82 (d, $J = 3.6$ Hz, 1H, furan *CH*), 6.65 (d, $J = 3.6$ Hz, 1H, furan *CH*), 6.03 (s, 2H, CH_2); ^{13}C NMR (101 MHz $CDCl_3$): δ 188.3, 156.7, 150.5, 148.3, 148.2, 140.3, 135.5, 131.4, 131.1, 130.2, 126.9, 124.1, 123.0, 119.9, 119.0, 117.4, 108.9, 107.4, 105.0, 101.5 (2 x C).

(*E*)-1-(benzo[*d*][1,3]dioxol-5-yl)-3-(5-(benzo[*d*][1,3]dioxol-5-yl)furan-2-yl)prop-2-en-1-one (7h): Yellow solid, 92% yield, 1H NMR (400 MHz $CDCl_3$): δ 7.69 (dd, $J = 8.2, 1.7$ Hz, 1H, *ArH*), 7.57 (d, $J = 15.2$ Hz, 1H, *CH*), 7.56 (d, $J = 1.7$ Hz, 1H, *ArH*), 7.42 (d, $J = 15.2$ Hz, 1H, *CH*), 7.30 (dd, $J = 8.1, 1.7$ Hz, 1H, *ArH*), 7.24 (d, $J = 1.6$ Hz, 1H, *ArH*), 6.91 (d, $J = 8.2$ Hz, 1H, *ArH*), 6.88 (d, $J = 8.1$ Hz, 1H, *ArH*), 6.77 (d, $J = 3.5$ Hz, 1H, furan *CH*), 6.63 (d, $J = 3.6$ Hz, 1H, furan *CH*), 6.07 (s, 2H, CH_2), 6.02 (s, 2H, CH_2); ^{13}C NMR (101 MHz $CDCl_3$): δ 187.6, 156.2, 151.6, 150.8, 148.3, 148.2, 148.1, 133.2, 130.0, 124.6, 124.3, 118.9 (2 x C), 118.0, 108.8, 108.4, 107.9, 107.2, 105.0, 101.8, 101.4; HRMS (ESI) 363.0855 ($[M + H]^+$), calcd. for $C_{21}H_{15}O_6^+$ 363.0863.

(*E*)-3-(5-([1,1'-biphenyl]-4-yl)furan-2-yl)-1-(3-bromophenyl)prop-2-en-1-one (7i): Yellow solid, 91% yield, 1H NMR (400 MHz $CDCl_3$): δ 8.19 (t, $J = 1.8$ Hz, 1H, *ArH*), 7.97 (dt, $J = 1.7, 7.9$ Hz, 1H, *ArH*), 7.87 (d, $J = 8.5$ Hz, 2H, *ArH*), 7.71 (ddd, $J = 1.0, 2.0, 7.9$ Hz, 1H, *ArH*), 7.69 (d, $J = 8.5$ Hz, 2H, *ArH*), 7.65 (d, $J = 7.6$ Hz, 2H, *ArH*), 7.64 (d, $J = 15.1$ Hz, 1H, *CH*), 7.47 (t, $J = 7.6$ Hz, 2H, *ArH*), 7.45 (d, $J = 15.1$ Hz, 1H, *CH*), 7.40 (t, $J = 7.8$ Hz, 1H, *ArH*), 7.38 (t, $J = 7.6$ Hz, 1H, *ArH*), 6.87 (d, $J = 3.4$, 1H, furan *CH*), 6.84 (d, $J = 3.4$, 1H, furan *CH*); ^{13}C NMR (101 MHz $CDCl_3$): δ 188.4, 156.6, 151.1, 141.5, 140.3, 140.2, 135.5, 131.4, 131.2, 130.2, 128.9 (2 x C), 128.6, 127.7, 127.6 (2 x C), 127.0 (2 x C), 126.9, 125.0 (2 x C), 123.0, 119.7, 117.9, 108.6.

(*E*)-3-(5-([1,1'-biphenyl]-4-yl)furan-2-yl)-1-(benzo[*d*][1,3]dioxol-5-yl)prop-2-en-1-one (7j): Yellow solid, 91% yield, 1H NMR (400 MHz $CDCl_3$): δ 7.85 (d, $J = 8.3$ Hz, 2H, *ArH*), 7.71 (dd, $J = 1.7, 8.1$ Hz, 1H, *ArH*), 7.68 (d, $J = 8.3$ Hz, 2H, *ArH*), 7.67-7.59 (m, 3H, *ArH* and *CH*) 7.57 (d, $J = 1.6$ Hz, 1H, *ArH*), 7.49 (d, $J = 15.1$ Hz, 1H, *CH*), 7.47 (t, $J = 7.5$ Hz, 2H, *ArH*), 6.92 (d, $J = 8.0$ Hz, 1H, *ArH*), 6.82 (s, 2H, 2 x furan *CH*), 6.08 (s, 2H, CH_2); ^{13}C NMR (101 MHz $CDCl_3$): δ 187.6, 156.1, 151.6, 151.4, 148.3, 141.3, 140.3, 133.2, 130.1, 128.9 (2 x C), 128.8, 127.7, 127.5 (2 x C), 127.4, 127.4, 127.0 (2 x C), 124.9 (2 x C), 124.6, 118.8, 118.4, 108.4 (2 x C), 101.9.

(*E*)-3-(5-bromofuran-2-yl)-1-(3-bromophenyl)prop-2-en-1-one (7k): To a stirred suspension of 5-aryl-2-furaldehyde (0.20 g, 1.1 mmol) in ethanol (5 mL) was added substituted acetophenone (1 equiv. 1.1 mmol) and aqueous sodium hydroxide (30% v/v, 5 mL) at room

1
2
3 temperature. The mixture was left stirring for 16 h before being diluted with water (10 mL).
4
5 The resulting suspension was isolated by filtration, washed with aqueous ethanol (1:1 v/v) and
6
7 dried to give the title compound (0.33 g, 0.93 mmol, 81%) as an off-white solid. ¹H NMR (400
8
9 MHz CDCl₃): δ 8.15 (t, *J* = 1.7 Hz, 1H, Ar*H*), 7.95 (d, *J* = 7.8 Hz, 1H, Ar*H*), 7.70 (dd, *J* = 0.9,
10
11 1.7, 8.0 Hz, 1H, Ar*H*), 7.49 (d, *J* = 15.2 Hz, 1H, CH), 7.38 (t, *J* = 7.8 Hz, 1H, Ar*H*), 7.36 (d, *J*
12
13 = 15.2 Hz, 1H, CH), 6.68 (d, *J* = 3.4 Hz, 1H, furan CH), 6.46 (d, *J* = 3.4 Hz, 1H, furan CH);
14
15 ¹³C NMR (101 MHz CDCl₃): δ 188.0, 153.4, 139.8, 135.7, 131.5, 130.2, 130.0, 127.0, 126.3,
16
17 123.0, 118.8 (2 x C), 114.8.

17
18 **(*E*)-1-(benzo[*d*][1,3]dioxol-5-yl)-3-(5-bromofuran-2-yl)prop-2-en-1-one (7l):** Yellow
19
20 solid, 97% yield. ¹H NMR (400 MHz CDCl₃): δ 7.67 (dd, *J* = 1.7, 8.2 Hz, 1H, Ar*H*), 7.53 (d,
21
22 *J* = 1.7 Hz, 1H, Ar*H*), 7.46 (d, *J* = 15.2 Hz, 1H, CH), 7.39 (d, *J* = 15.2 Hz, 1H, CH), 6.90 (d, *J*
23
24 = 8.2 Hz, 1H, Ar*H*), 6.63 (d, *J* = 3.4 Hz, 1H, furan CH), 6.44 (d, *J* = 3.4 Hz, 1H, furan CH),
25
26 6.06 (s, 2H, CH₂); ¹³C NMR (101 MHz CDCl₃): δ 187.4, 153.7, 151.8, 148.4, 132.8, 128.9,
27
28 125.6, 124.8, 119.4, 117.9, 114.5, 108.4, 108.0, 101.9.

27
28 **General Procedure for Preparations of Compounds 8b-8l.** To a suspension of chalcone
29
30 (0.10 g) in ethanol (1.5 mL) was added hydrazine hydrate (0.028 mL, 60 % in H₂O). The
31
32 reaction vessel was purged with argon and then heated with microwave irradiation (300 W of
33
34 max. power) to 70 °C. The pressure limit was set at 190 *psi*. Once the desired temperature was
35
36 reached over 5 minutes, heating was continued for a further hour to maintain temperature. The
37
38 mixture was then allowed to cool to room temperature before being concentrated under reduced
39
40 pressure before being recrystallised from ethanol to give pure pyrazolines.

39
40 **3-(benzo[*d*][1,3]dioxol-5-yl)-5-(5-phenylfuran-2-yl)-4,5-dihydro-1*H*-pyrazole (8b):**
41
42 Off-white solid, 80% yield, ¹H NMR (400 MHz CDCl₃): δ 7.63-7.61 (m, 2H, Ar*H*), 7.36 (t, *J*
43
44 = 7.6 Hz, 2H, 2 x Ar*H*), 7.32 (d, *J* = 1.5 Hz, 1H, Ar*H*), 7.26-7.22 (m, 1H, Ar*H*), 7.08 (dd, *J* =
45
46 1.7, 8.2 Hz, 1H, Ar*H*), 6.82 (d, *J* = 8.0 Hz, 1H, Ar*H*), 6.57 (d, *J* = 3.4, 1H, furan CH), 6.32 (d,
47
48 *J* = 3.4 Hz, 1H, furan CH), 5.99 (s, 2H, CH₂), 5.01 (dd, *J* = 7.7, 10.2 Hz, 1H, CH), 3.37 (dd, *J*
49
50 = 10.2, 16.2 Hz, 1H, CHH), 3.27 (dd, *J* = 7.8, 16.2 Hz, 1H, CHH); ¹³C NMR (101 MHz CDCl₃):
51
52 δ 154.1, 153.8, 152.4, 148.6, 148.1, 130.5, 128.7 (2 x C), 127.5, 127.0, 123.7 (2 x C), 120.8,
53
54 108.2, 108.1, 106.1, 105.6, 101.3, 57.3, 38.0; HRMS (ESI) 333.1228 ([M + H]⁺), calcd. for
55
56 C₂₀H₁₇N₂O₃⁺ 333.1234.

55
56 **3-(3-bromophenyl)-5-(5-(3-chlorophenyl)furan-2-yl)-4,5-dihydro-1*H*-pyrazole (8c):**
57
58 White powder, 70% yield, ¹H NMR (400 MHz CDCl₃): δ 7.85 (t, *J* = 1.8 Hz, 1H, Ar), 7.62 (dt,
59
60 *J* = 1.3, 7.8 Hz, 1H, Ar*H*), 7.60 (t, *J* = 1.7 Hz, 1H, Ar*H*), 7.50-7.48 (m, 2H, 2 x Ar*H*), 7.29 (t,
J = 8.0 Hz, 1H, Ar*H*), 7.27 (t, *J* = 7.9 Hz, 1H, Ar*H*), 7.22 (ddd, *J* = 1.2, 1.9, 8.0 Hz, 1H, Ar*H*),

6.60 (d, $J = 3.4$ Hz, 1H, furan *CH*), 6.35 (d, $J = 3.4$ Hz, 1H, *ArH*), 5.07 (t, $J = 9.2$ Hz, 1H, *CH*), 3.41 (dd, $J = 10.4, 16.2$ Hz, 1H, *CHH*), 3.30 (dd, $J = 7.9, 16.2$ Hz, 1H, *CHH*); ^{13}C NMR (101 MHz CDCl_3): δ 154.2, 152.5, 151.3, 134.7, 134.5, 132.1, 132.0, 130.1, 130.0, 129.1, 127.4, 124.7, 123.7, 122.8, 121.8, 108.6, 106.8, 57.4, 37.6; HRMS (ESI) 401.0051 ($[\text{M} + \text{H}]^+$), calcd. for $\text{C}_{19}\text{H}_{15}\text{BrClN}_2\text{O}^+$ 401.0051.

3-(benzo[*d*][1,3]dioxol-5-yl)-5-(5-(3-chlorophenyl)furan-2-yl)-4,5-dihydro-1*H*-pyrazole (8d): White solid, 59 % yield, ^1H NMR (400 MHz CDCl_3): δ 7.61 (t, $J = 1.8$ Hz, 1H, *ArH*), 7.49 (dt, $J = 7.7, 1.3$ Hz, 1H, *ArH*), 7.31 (d, $J = 1.6$ Hz, 1H, *ArH*), 7.88 (t, $J = 7.9$ Hz, 1H, *ArH*) 7.21 (ddd, $J = 1.1, 1.9, 7.9$ Hz, 1H, *ArH*), 7.07 (dd, $J = 8.1, 1.7$ Hz, 1H, *ArH*), 6.82 (d, $J = 8.1$ Hz, 1H, *ArH*), 6.60 (d, $J = 3.4$ Hz, 1H, furan *CH*), 6.33 (d, $J = 3.3$ Hz, 1H, furan *CH*), 6.00 (s, 2H, CH_2), 4.99 (dd, $J = 10.3, 8.0$ Hz, 1H, *CH*), 3.37 (dd, $J = 16.1, 10.3$ Hz, 1H, *CHH*), 3.25 (dd, $J = 16.1, 7.9$ Hz, 1H, *CHH*); ^{13}C NMR (101 MHz CDCl_3): δ 154.9, 152.3, 151.9, 148.5, 148.1, 134.7, 132.2, 130.0, 127.3, 127.0, 123.7, 121.7, 120.7, 108.3, 108.1, 106.8, 106.1, 101.3, 57.4, 38.1; HRMS (ESI) 367.0827 ($[\text{M} + \text{H}]^+$), calcd. for $\text{C}_{20}\text{H}_{16}\text{ClN}_2\text{O}_3^+$ 367.0844.

3-(3-bromophenyl)-5-(5-(4-methoxyphenyl)furan-2-yl)-4,5-dihydro-1*H*-pyrazole (8e): Off-white solid, 68% yield, ^1H NMR (400 MHz CDCl_3): δ 7.85 (s, 1H, *ArH*), 7.62 (d, $J = 8.0$ Hz, 1H, *ArH*), 7.55 (d, $J = 8.9$ Hz, 2H, 2 x *ArH*), 7.47 (d, $J = 8.0$ Hz, 1H, *ArH*), 7.26 (t, $J = 8.0$ Hz, 1H, *ArH*), 6.90 (d, $J = 8.9$ Hz, 2H, 2 x *ArH*), 6.43 (d, $J = 3.4$ Hz, 1H, furan *CH*), 6.29 (d, $J = 3.4$ Hz, 1H, furan *CH*), 5.04 (dd, $J = 7.8, 10.2$ Hz, 1H, *CH*), 3.82 (s, 3H, CH_3), 3.66 (dd, $J = 10.2, 16.2$ Hz, 1H, *CHH*), 3.28 (dd, $J = 7.7, 16.2$ Hz, 1H, *CHH*); ^{13}C NMR (101 MHz CDCl_3): δ 159.2, 154.0, 153.1, 150.4, 134.7, 131.7, 130.1, 129.0, 125.2 (2 x C), 124.6, 123.6, 122.8, 114.1, 108.2, 104.0, 57.5, 55.3, 37.5; HRMS (ESI) 397.0540 ($[\text{M} + \text{H}]^+$), calcd. for $\text{C}_{20}\text{H}_{18}\text{BrN}_2\text{O}_2^+$ 397.0546.

3-(benzo[*d*][1,3]dioxol-5-yl)-5-(5-(4-methoxyphenyl)furan-2-yl)-4,5-dihydro-1*H*-pyrazole (8f): Off-white solid, 62% yield, ^1H NMR (400 MHz CDCl_3): δ 7.55 (d, $J = 8.9$ Hz, 2H, 2 x *ArH*), 7.32 (d, $J = 1.7$ Hz, 1H, *ArH*), 7.08 (dd, $J = 1.7, 8.4$ Hz, 1H, *ArH*), 6.90 (d, $J = 8.9$ Hz, 2H, 2 x *ArH*), 6.82 (d, $J = 8.0$ Hz, 1H, *ArH*), 6.43 (d, $J = 3.4$ Hz, 1H, furan *CH*), 6.29 (d, $J = 3.4$ Hz, 1H, furan *CH*), 5.99 (s, 2H, CH_2), 5.00 (dd, $J = 7.6, 10.1$ Hz, 1H, *CH*), 3.82 (s, 3H, CH_3), 3.36 (dd, $J = 10.2, 16.2$ Hz, 1H, *CHH*), 3.27 (dd, $J = 7.6, 16.2$ Hz, 1H, *CHH*); ^{13}C NMR (101 MHz CDCl_3): δ 159.1, 153.8, 153.5, 152.0, 148.5, 148.1, 127.1, 125.2 (2 x C), 123.7, 120.7, 114.1 (2 x C), 108.1, 108.0, 106.1, 104.0, 101.3, 57.3, 55.3, 38.0; HRMS (ESI) 363.1324 ($[\text{M} + \text{H}]^+$), calcd. for $\text{C}_{21}\text{H}_{19}\text{N}_2\text{O}_4^+$ 363.1339.

1
2
3
4
5
6
7
8
9
10
11
12
13
14
15
16
17
18
3-(benzo[*d*][1,3]dioxol-5-yl)-5-(5-(benzo[*d*][1,3]dioxol-5-yl)furan-2-yl)-4,5-dihydro-1*H*-pyrazole (8h): Yellow solid, 70% yield, ¹H NMR (400 MHz CDCl₃): δ 7.31 (d, *J* = 1.7 Hz, 1H, Ar*H*), 7.13 (dd, *J* = 1.7, 8.2 Hz, 1H, Ar*H*), 7.08 (d, *J* = 1.7 Hz, 1H, Ar*H*), 7.07 (dd, *J* = 1.7, 8.2 Hz, 1H, Ar*H*), 6.82 (d, *J* = 8.2 Hz, 1H, Ar*H*), 6.80 (d, *J* = 8.2 Hz, 1H, Ar*H*), 6.41 (d, *J* = 3.3 Hz, 1H, furan *CH*), 6.29 (d, *J* = 3.3 Hz, 1H, furan *CH*), 5.99 (s, 2H, CH₂), 5.97 (s, 2H, CH₂), 4.99 (dd, *J* = 7.8, 10.1 Hz, 1H, *CH*), 3.35 (dd, *J* = 10.2, 16.2 Hz, 1H, *CHH*), 3.26 (dd, *J* = 7.9, 16.2 Hz, 1H, *CHH*); ¹³C NMR (101 MHz CDCl₃): δ 153.7, 153.3, 152.7, 148.6, 148.1, 148.0, 147.1, 126.9, 125.0, 120.8, 117.7, 108.6, 108.3, 108.1, 106.2, 104.5 (2 x C), 101.3, 101.1, 57.2, 38.0; HRMS (ESI) 377.1109 ([*M* + *H*]⁺), calcd. for C₂₁H₁₇N₂O₅⁺ 377.1132.

19
20
21
22
23
24
25
26
27
28
29
30
31
32
33
34
5-(5-([1,1'-biphenyl]-4-yl)furan-2-yl)-3-(3-bromophenyl)-4,5-dihydro-1*H*-pyrazole (8i): Off-white solid, 87% yield, ¹H NMR (400 MHz CDCl₃): δ 7.86 (t, *J* = 1.7 Hz, 1H, Ar*H*), 7.69 (d, *J* = 7.9 Hz, 2H, 2 x Ar*H*), 7.64-7.60 (m, 5H, Ar*H*), 7.48 (ddd, *J* = 1.2, 1.6, 8.0 Hz, 1H, Ar*H*), 7.46-7.43 (m, 2H, 2 x Ar*H*), 7.35 (t, *J* = 7.43 Hz, 1H, Ar*H*), 7.27 (t, *J* = 7.9 Hz, 1H, Ar*H*), 6.61 (d, *J* = 3.4 Hz, 1H, furan *CH*), 6.35 (d, *J* = 3.4 Hz, 1H furan *CH*), 5.08 (dd, *J* = 7.5, 10.1 Hz, 1H, *CH*), 3.40 (dd, *J* = 10.3, 16.2 Hz, 1H, *CHH*), 3.32 (dd, *J* = 7.6, 16.2 Hz, 1H, *CHH*); ¹³C NMR (101 MHz CDCl₃): δ 153.9, 153.7, 150.8, 140.5, 140.2, 134.6, 131.9, 130.1, 129.4, 129.1, 128.8 (2 x C), 127.4 (3 x C), 126.9 (2 x C), 124.6, 124.1 (2 x C), 122.8, 108.5, 105.8, 57.5, 37.6; HRMS (ESI) 443.0733 ([*M* + *H*]⁺), calcd. for C₂₅H₂₀BrN₂O⁺ 443.0754.

35
36
37
38
39
40
41
42
43
44
45
46
47
48
49
50
5-(5-([1,1'-biphenyl]-4-yl)furan-2-yl)-3-(benzo[*d*][1,3]dioxol-5-yl)-4,5-dihydro-1*H*-pyrazole (8j): Off-white solid, 78% yield, ¹H NMR (400 MHz CDCl₃): δ 7.70-7.69 (m, 2H, 2 x Ar*H*), 7.62-7.64 (m, 4H, 4 x Ar*H*), 7.45 (t, *J* = 7.5 Hz, 2H, 2 x Ar*H*), 7.36 (d, *J* = 7.5 Hz, 1H, Ar*H*), 7.33 (d, *J* = 1.6 Hz, 1H, Ar*H*), 7.09 (dd, *J* = 1.4, 7.9 Hz, 1H, Ar*H*), 6.83 (d, *J* = 8.1 Hz, 1H, Ar*H*), 6.61 (d, *J* = 3.4 Hz, 1H, furan *CH*), 6.34 (d, *J* = 3.4 Hz, 1H, furan *CH*), 6.00 (s, 2H, CH₂), 5.02 (dd, *J* = 7.8, 10.2 Hz, 1H, *CH*), 3.38 (dd, *J* = 10.2, 16.1 Hz, 1H, *CHH*), 3.29 (dd, *J* = 7.7, 16.1 Hz, 1H, *CHH*); ¹³C NMR (101 MHz CDCl₃): δ 154.3, 153.6, 152.2, 148.5, 148.1, 140.5, 140.1, 129.5, 128.8 (2 x C), 127.4, 127.3 (2 x C), 127.0, 126.9 (2 x C), 124.1 (2 x C), 120.7, 108.3, 108.1, 106.1, 105.8, 101.3, 57.4, 38.0; HRMS (ESI) 409.1539 ([*M* + *H*]⁺), calcd. for C₂₆H₂₁N₂O₃⁺ 409.1547.

51
52
53
54
55
56
57
58
59
60
5-(5-bromofuran-2-yl)-3-(3-bromophenyl)-4,5-dihydro-1*H*-pyrazole (8k): Off-white solid, 70% yield, ¹H NMR (400 MHz CDCl₃): δ 7.81 (t, *J* = 1.9 Hz, 1H, Ar*H*), 7.59 (d, *J* = 7.8 Hz, 1H, Ar*H*), 7.47 (d, *J* = 8.0 Hz, 1H, Ar*H*), 7.25 (t, *J* = 7.8 Hz, 1H, Ar*H*), 6.24 (s, 2H, 2 x furan *CH*), 4.96 (dd, *J* = 7.8, 15.8 Hz, 1H, *CH*), 3.35 (dd, *J* = 10.4, 16.2 Hz, *CHH*), 3.20 (dd, *J* = 7.6, 16.2 Hz, 1H, *CHH*); ¹³C NMR (101 MHz CDCl₃): δ 134.8, 133.1, 131.0, 130.7, 129.6, 126.0, 125.2, 123.4, 114.1, 112.8, 100.2, 54.4, 38.1 (total 2 atoms not observed).

3-(benzo[*d*][1,3]dioxol-5-yl)-5-(5-bromofuran-2-yl)-4,5-dihydro-1*H*-pyrazole (8l): Off-white solid, 71% yield, ¹H NMR (400 MHz CDCl₃): δ 7.29 (d, *J* = 1.6 Hz, 1H, Ar*H*), 7.05 (dd, *J* = 1.7, 8.1 Hz, 1H, Ar*H*), 6.81 (d, *J* = 8.1 Hz, 1H, Ar*H*), 6.25 (d, *J* = 3.4 Hz, 1H, furan *CH*), 6.23 (d, *J* = 3.4 Hz, 1H, furan *CH*), 5.99 (s, 2H, CH₂), 4.93 (dd, *J* = 7.8, 10.3 Hz, 1H, *CH*), 3.33 (dd, *J* = 10.3, 16.3 Hz, 1H, CHH), 3.19 (dd, *J* = 7.8, 16.3 Hz, 1H, CHH); ¹³C NMR (101 MHz CDCl₃): δ 156.2, 153.3, 148.9, 148.2, 126.7, 121.8, 121.1, 112.2, 109.3, 108.3, 106.3, 101.5, 57.1, 38.1.

General Procedure for Preparations of Compounds 9a-9j. To a suspension of chalcone (0.100 g) and elemental sulfur (0.022 g, 3 eq.) in ethanol (1.00 mL) was added hydrazine hydrate (0.046 mL, 60 % in H₂O). The reaction vessel was purged with argon and then heated with microwave irradiation (300 W of max. power) to 150 °C. The pressure limit was set at 190 *psi*. Once the desired temperature was reached over 5 minutes, heating was continued for a further two hours to maintain temperature. The mixture was then allowed to cool to room temperature before being concentrated under reduced pressure, redissolved in ethyl acetate and filtered to remove solid sulfur powder. The filtrate was then concentrated before being purified by flash chromatography.

3-(3-bromophenyl)-5-(5-phenylfuran-2-yl)-1*H*-pyrazole (9a): Off-white solid, 22% yield, ¹H NMR (400 MHz DMSO-*d*₆): δ 8.08 (t, *J* = 1.8 Hz, 1H, Ar*H*), 7.88 (dt, *J* = 1.3, 7.8 Hz, 1H, Ar*H*), 7.85-7.83 (m, 2H, Ar*H*), 7.54 (ddd, *J* = 0.9, 1.9, 8.0 Hz, 1H, Ar*H*), 7.48-7.44 (m, 2H, Ar*H*), 7.42 (t, *J* = 7.8 Hz, 1H, Ar*H*), 7.34-7.30 (m, 1H, Ar*H*), 7.23 (s, 1H, *CH*), 7.04 (d, *J* = 3.5 Hz, 1H, furan *CH*), 6.91 (d, *J* = 3.5 Hz, 1H, furan *CH*); ¹³C NMR (101 MHz DMSO-*d*₆): δ 158.5, 152.9, 131.5, 131.0, 130.4, 129.4, 128.1, 124.6, 124.0, 122.8, 109.0, 108.2, 100.3 (3 carbon atoms not observed); HRMS (ESI) 365.0282 ([*M* + *H*]⁺), calcd. for C₁₉H₁₄BrN₂O⁺ 365.0284.

3-(benzo[*d*][1,3]dioxol-5-yl)-5-(5-phenylfuran-2-yl)-1*H*-pyrazole (9b): Off-white solid, 19% yield, ¹H NMR (400 MHz DMSO-*d*₆): δ 7.82 (d, *J* = 7.8 Hz, 2H, Ar*H*), 7.46 (t, *J* = 7.8 Hz, 2H, Ar*H*), 7.41 (d, *J* = 1.6 Hz, 1H, Ar*H*), 7.36 (dd, *J* = 1.6, 8.0 Hz, 1H, Ar*H*), 7.32 (t, *J* = 7.4 Hz, 1H, Ar*H*), 7.07 (d, *J* = 3.6 Hz, 1H, furan *CH*), 7.03 (s, 1H, *CH*), 7.00 (d, *J* = 7.9 Hz, 1H, Ar*H*), 6.86 (d, *J* = 3.6 Hz, 1H, furan *CH*), 6.07 (s, 2H, CH₂); ¹³C NMR (101 MHz DMSO-*d*₆): δ 152.7, 148.3, 147.5, 130.5, 129.4 (2 x C), 128.0, 123.9 (2 x C), 119.5, 109.1, 108.6, 108.2, 106.2, 101.7, 99.4; HRMS (ESI) 331.1060 ([*M* + *H*]⁺), calcd. for C₂₀H₁₅N₂O₃⁺ 331.1077.

3-(3-bromophenyl)-5-(5-(3-chlorophenyl)furan-2-yl)-1*H*-pyrazole (9c): Off-white solid, 15% yield, ¹H NMR (400 MHz DMSO-*d*₆): δ 8.07 (t, *J* = 1.7 Hz, 1H, Ar*H*), 7.92 (t, *J* = 1.7 Hz, 1H, Ar*H*), 7.88 (dt, *J* = 1.2, 7.7 Hz, 1H, Ar*H*), 7.80 (dt, *J* = 1.3, 7.8 Hz, 1H, Ar*H*), 7.55

(ddd, $J = 1.0, 1.9, 8.0$ Hz, 1H, ArH), 7.48 (t, $J = 7.9$ Hz, 1H, ArH), 7.42 (t, $J = 7.9$ Hz, 1H, ArH), 7.37 (ddd, $J = 1.0, 2.0, 8.0$ Hz, 1H, ArH), 7.27 (s, 1H, CH), 7.22 (d, $J = 3.6$ Hz, 1H, furan CH), 6.94 (d, $J = 3.6$ Hz, 1H, furan CH); ^{13}C NMR (101 MHz DMSO- d_6): δ 150.9, 133.9, 131.9, 131.1, 130.9, 130.6, 127.7, 127.3, 124.2, 123.0, 122.3, 122.1, 109.3, 108.7, 100.1 (total 4 carbon atoms not observed); HRMS (ESI) 398.9886 ($[\text{M} + \text{H}]^+$), calcd. for $\text{C}_{19}\text{H}_{13}\text{BrClN}_2\text{O}^+$ 398.9894.

3-(benzo[*d*][1,3]dioxol-5-yl)-5-(5-(3-chlorophenyl)furan-2-yl)-1H-pyrazole (9d): Off-white solid, 31% yield, ^1H NMR (400 MHz DMSO- d_6): δ 7.88 (t, $J = 1.7$ Hz, 1H, ArH), 7.77 (dt, $J = 1.2, 8.0$ Hz, 1H, ArH), 7.47 (t, $J = 7.9$ Hz, 1H, ArH), 7.41 (d, $J = 1.5$ Hz, 1H, ArH), 7.37-7.34 (m, 2H, 2 x ArH), 7.19 (d, $J = 3.5$ Hz, 1H, furan CH), 7.07 (s, 1H, CH), 7.00 (d, $J = 8.2$ Hz, 1H, ArH), 6.89 (d, $J = 3.5$ Hz, 1H, furan CH), 6.06 (s, 2H, CH_2); ^{13}C NMR (101 MHz DMSO- d_6): δ 150.6, 147.8, 147.1, 133.9, 132.0, 130.9, 127.2, 122.9, 122.0, 119.1, 109.3, 108.7, 108.3, 105.7, 101.2, 99.2 (total 4 carbon atoms not observed); HRMS (ESI) 365.0685 ($[\text{M} + \text{H}]^+$), calcd. for $\text{C}_{20}\text{H}_{14}\text{ClN}_2\text{O}_3^+$ 365.0688.

3-(3-bromophenyl)-5-(5-(4-methoxyphenyl)furan-2-yl)-1H-pyrazole (9e): Off-white solid, 21% yield, ^1H NMR (400 MHz DMSO- d_6): δ 8.06 (t, $J = 1.7$, 1H, ArH), 7.87 (dt, $J = 0.9, 7.8$ Hz, 1H, ArH), 7.76 (d, $J = 8.8$ Hz, 2H, 2 x ArH), 7.54 (ddd, $J = 0.9, 1.8, 8.0$ Hz, 1H, ArH), 7.42 (t, $J = 7.9$ Hz, 1H, ArH), 7.18 (s, 1H, CH), 7.03 (d, $J = 8.9$ Hz, 2H, 2 x ArH), 6.92 (d, $J = 3.4$ Hz, 1H, furan CH), 6.87 (d, $J = 3.4$ Hz, 1H, furan CH), 3.80 (s, 3H, CH_3); ^{13}C NMR (101 MHz DMSO- d_6): δ 159.0, 158.6, 131.1, 130.6, 127.7, 125.2 (2 x C), 124.2, 122.9, 114.5 (2 x C), 108.6, 106.0, 99.6, 55.3 (total 5 carbon atoms not observed); HRMS (ESI) 395.0373 ($[\text{M} + \text{H}]^+$), calcd. for $\text{C}_{20}\text{H}_{16}\text{BrN}_2\text{O}_2^+$ 395.0390.

3-(benzo[*d*][1,3]dioxol-5-yl)-5-(5-(4-methoxyphenyl)furan-2-yl)-1H-pyrazole (9f): Off-white solid, 13% yield, ^1H NMR (400 MHz DMSO- d_6): δ 7.74 (d, $J = 8.9$ Hz, 2H, 2 x ArH), 4.41 (d, $J = 1.6$ Hz, 1H, ArH), 7.36 (dd, $J = 1.6, 7.9$ Hz, 1H, ArH), 7.03 (d, $J = 8.9$ Hz, 2H, 2 x ArH), 7.00 (d, $J = 7.9$ Hz, 1H, ArH), 6.99 (s, 1H, CH), 6.90 (d, $J = 3.5$ Hz, 1H, furan CH), 6.82 (d, $J = 3.5$ Hz, 1H, furan CH), 6.06 (s, 2H, CH_2), 3.80 (s, 3H, CH_3); ^{13}C NMR (101 MHz DMSO- d_6): δ 159.3, 152.9, 148.2, 147.5, 125.5 (2 x C), 123.4, 119.4, 114.8 (2 x C), 109.1, 108.6, 106.4, 106.1, 101.6, 99.2, 55.7 (total 4 carbon atoms not observed); HRMS (ESI) 361.1160 ($[\text{M} + \text{H}]^+$), calcd. for $\text{C}_{21}\text{H}_{17}\text{N}_2\text{O}_4^+$ 361.1182.

5-(5-(benzo[*d*][1,3]dioxol-5-yl)furan-2-yl)-3-(3-bromophenyl)-1H-pyrazole (9g): Off-white solid, 29% yield, ^1H NMR (400 MHz DMSO- d_6 + TFA): δ 8.05 (s, 1H, ArH), 7.86 (d, $J = 7.5$ Hz, 1H, ArH), 7.53 (d, $J = 7.8$ Hz, 1H, ArH), 7.42-7.39 (m, 2H, 2 x ArH), 7.35 (d, $J = 7.5$ Hz, 1H, ArH), 7.19 (s, 1H, CH), 7.01 (d, $J = 7.8$ Hz, 1H, ArH), 6.95 (d, $J = 3.1$ Hz, 1H,

furan *CH*), 6.86 (d, $J = 3.1$ Hz, 1H, furan *CH*), 6.07 (s, 2H, CH_2); ^{13}C NMR (101 MHz DMSO-d₆): δ 152.5, 148.0, 147.0, 134.1, 131.1, 130.6, 127.7, 124.4, 124.2, 122.4, 117.7, 108.9, 108.7, 106.7, 104.3, 101.4, 99.7; HRMS (ESI) 409.0169 ($[M + H]^+$), calcd. for $C_{20}H_{14}BrN_2O_3^+$ 409.0182.

3-(benzo[*d*][1,3]dioxol-5-yl)-5-(5-(benzo[*d*][1,3]dioxol-5-yl)furan-2-yl)-1*H*-pyrazole

(9h): Off-white solid, 13% yield, 1H NMR (400 MHz DMSO-d₆): δ 7.40 (d, $J = 1.6$ Hz, 2H, 2 x *ArH*), 7.35 (dd, $J = 1.6, 8.0$ Hz, 1H, *ArH*), 7.33 (dd, $J = 1.6, 8.0$ Hz, 1H, *ArH*), 7.02 (s, 1H, *CH*), 7.01 (d, $J = 8.0$ Hz, 1H, *ArH*), 6.99 (d, $J = 8.0$ Hz, 1H, *ArH*), 6.94 (d, $J = 3.5$ Hz, 1H, furan *CH*), 6.82 (d, $J = 3.5$ Hz, 1H, furan *CH*), 6.07 (s, 2H, CH_2), 6.06 (s, 2H, CH_2); ^{13}C NMR (101 MHz DMSO-d₆): δ 148.4, 148.2, 147.5, 124.9, 119.4, 117.9, 109.3, 109.1, 108.5, 107.0, 106.1, 104.6, 101.7, 101.6, 99.3 (total 5 carbon atoms not observed); HRMS (ESI) 375.0976 ($[M + H]^+$), calcd. for $C_{21}H_{15}N_2O_5^+$ 375.0976.

5-(5-([1,1'-biphenyl]-4-yl)furan-2-yl)-3-(3-bromophenyl)-1*H*-pyrazole (9i): Off-white solid, 42% yield, 1H NMR (400 MHz DMSO-d₆): δ 13.57 (bs, 1H, *NH*), 8.09 (s, 1H, *ArH*), 7.93 (d, $J = 8.4$ Hz, 2H, 2 x *ArH*), 7.89 (d, $J = 7.8$ Hz, 1H, *ArH*), 7.79-7.73 (m, 4H, 4 x *ArH*), 7.55 (d, $J = 7.8$ Hz, 1H, *ArH*), 7.49 (t, $J = 7.5$ Hz, 2H, 2 x *ArH*), 7.47 (t, $J = 7.8$ Hz, 1H, *ArH*), 7.38 (t, $J = 7.5$ Hz, 1H, *ArH*), 7.25 (s, 1H, *CH*), 7.15 (d, $J = 3.5$ Hz, 1H, furan *CH*), 6.94 (d, $J = 3.5$ Hz, 1H, furan *CH*); ^{13}C NMR (101 MHz DMSO-d₆): δ 152.7, 139.9, 139.6, 131.5, 131.0, 129.5 (2 x C), 128.1 (2 x C), 127.6 (2 x C), 127.0 (2 x C), 124.6 (3 x C), 124.5, 122.8, 108.5, 100.4 (total 6 carbon atoms not observed); HRMS (ESI) 441.0592 ($[M + H]^+$), calcd. for $C_{26}H_{19}N_2O_3^+$ 441.0597.

5-(5-([1,1'-biphenyl]-4-yl)furan-2-yl)-3-(benzo[*d*][1,3]dioxol-5-yl)-1*H*-pyrazole (9j):

Off-white solid, 29% yield, 1H NMR (400 MHz DMSO-d₆): δ 7.91 (d, $J = 8.4$ Hz, 1H, *ArH*), 7.78 (m, 4H, 4 x *ArH*), 7.49 (t, $J = 7.8$ Hz, 2H, 2 x *ArH*), 7.42 (d, $J = 1.66$, 1H, *ArH*), 7.38 (tt, $J = 1.2, 7.3$ Hz, 1H, *ArH*), 7.37 (dd, $J = 1.7, 7.9$ Hz, 1H, *ArH*), 7.14 (d, $J = 3.5$ Hz, 1H, furan *CH*), 7.06 (s, 1H, *CH*), 7.01 (d, $J = 7.9$ Hz, 1H, *ArH*), 6.89 (d, $J = 3.5$ Hz, 1H, furan *CH*), 6.07 (s, 2H, CH_2); ^{13}C NMR (101 MHz DMSO-d₆): δ 152.4, 148.3, 147.5, 139.9, 139.5, 129.6, 129.5 (2 x C), 128.1, 127.6 (2 x C), 127.0 (2 x C), 124.5 (2 x C), 119.5, 109.1, 108.5, 106.2, 101.7, 99.4 (total 5 carbon atoms not observed); HRMS (ESI) 407.1379 ($[M + H]^+$), calcd. for $C_{26}H_{19}N_2O_3^+$ 407.1390.

3-(benzo[*d*][1,3]dioxol-5-yl)-5-(3-bromophenyl)-1*H*-pyrazole (1): Yellow powder, 65% yield, 1H NMR (400 MHz DMSO-d₆): δ 8.01 (t, $J = 1.7$ Hz, 1H, *ArH*), 7.82 (dt, $J = 1.3, 7.8$ Hz, 1H, *ArH*), 7.51 (ddd, $J = 0.9, 1.9, 7.9$ Hz, 1H, *ArH*), 7.40 (t, $J = 7.9$ Hz, 1H, *ArH*), 7.38 (d, $J = 1.6$ Hz, 1H, *ArH*), 7.33 (dd, $J = 1.7, 8.1$ Hz, 1H, *ArH*), 7.20 (s, 1H, *ArH*), 7.01 (d, $J = 8.1$

1
2
3 Hz, 1H, ArH), 6.06 (s, 2H, CH₂); ¹³C NMR (101 MHz DMSO-d₆): δ 158.6, 158.2, 147.9,
4 147.1, 134.5, 131.0, 130.4, 127.5, 124.0, 122.3, 119.0, 116.7, 108.8, 105.6, 101.3, 99.9.

5
6 ***In Vitro Biological Evaluation. Expression and Purification of α-Synuclein.*** *Escherichia*
7 *coli* BL21 (DE3) cells containing the human α-syn gene inserted into a pET-22b (+) vector
8 (Novagen, Merck, MA, USA) were induced with 1 mM isopropyl β-D-1-
9 thiogalactopyranoside. α-syn was first purified following a non-chromatographic protocol
10 reported by Volles and Lansbury.³⁶ Further purification using anion exchange followed
11 protocols reported by Ventura and co-workers.³⁷

12
13 ***In Vitro Inhibition of α-Synuclein Aggregation.*** A stock solution of ThT (5 mM) in glycine-
14 NaOH buffer (pH 8.0) was prepared and used with homogenous monomeric α-syn, made using
15 commonly employed protocols described by Rahimi et al.³⁸ Inhibition of α-syn aggregation
16 was performed by incubation of a mixture of α-syn monomers (80 μM) suspended in
17 aggregation buffer (20 mM Tris-HCl, pH 7.4, 150 mM NaCl and 0.05% NaN₃) with or without
18 candidate inhibitor compounds (80 μM and 400 μM) at 37°C with constant shaking (1000 rpm
19 in a thermomixer) for 48 h. For each treatment group, pre-incubated α-syn samples (60 μL)
20 were mixed with a ThT solution (240 μL, 50 μM) for 10 min, the solution was dispensed in
21 triplicate (n=3) into 96-well plates which were analysed using a fluorimeter (ex. 440 nm/em.
22 500 nm). The fluorescence intensity of samples were compared to an untreated negative control
23 and a positive control treated with epigallocatechin gallate (EGCG, 80 μM and 400 μM) to
24 obtain percentage inhibition values.

25
26 ***Dot blot assay:*** Briefly, samples (2 μL) were immobilized on nitrocellulose membrane
27 (Amersham Protran, GE Healthcare) and were dried at rt. The membrane was blocked at rt for
28 1 h using 3% bovine serum albumin (BSA) and then was washed with Tris-buffered saline
29 (TBST, 0.05% Tween 20, 50 mM Tris-HCl, 150 mM NaCl, pH 7.5). The membranes were
30 incubated overnight at 4 °C with anti-α-Synuclein antibody (1:2000, BD Biosciences)³⁹
31 and anti-α-Synuclein filament antibody (1:8,000, Abcam).⁴⁰ The membranes were washed with
32 TBST and then incubated with secondary anti-mouse and anti-rabbit IgG (1:20,000, Thermo
33 Scientific) at rt for 2 h. The blots were incubated further with ECL reagent (Millipore) for 5
34 min, before being developed.

35
36
37
38
39
40
41
42
43
44
45
46
47
48
49
50
51
52
53
54
55
56
57
58
59
60
Molecular modelling: Molecular docking analysis was carried out using Schrodinger software
package⁴¹ with (and without) Induce fit docking option in Glide module. Geometry
optimization of initial 3D structures of all the compounds was performed using OPLS3 force

1
2
3 field.⁴² The structures of designed compounds were prepared using LigPrep module of Maestro
4 software. To prepare the macromolecular environment, the protein preparation wizard of
5 maestro software was employed. The coordinates for dimer of β -sheet were taken from the
6 hTau homodimer protein identified by PDB Id 4E0M, which consists of four chains A, B, C
7 and D respectively, in which A, B and C, D were arranged in antiparallel manner via hydrogen
8 bonds to form aggregates to each other. Water molecules, inorganic phosphate, chain A and
9 chain B of β -sheet were deleted. The amino acids present in the dimer are GLN, GLU9, ILE4,
10 LYS13, PHE10, SER1, TYR6 and VAL5 respectively between C and D chains.
11
12

13 SiteMap⁴³ module in association with Glide software was used to identify the cavity employed
14 in performing molecular docking. The grid for molecular docking was generated with outer
15 and inner box of 26 Å and 10 Å respectively using auto option in Induced Fit Docking (IFD)
16 module of Maestro software. The receptor van der Waals and ligand van der Waals scaling
17 were kept to 0.50 and for selected 20 poses. Refinement of conformation of the residues during
18 IFD was done on residues within 5.0 Å. SP precision mode was used for IFD purpose. Prime
19 MMGBSA option within application tools of Maestro package was used to estimate the binding
20 free energies between the docked compounds and macromolecular environment which
21 indicated no conformational interference. The validation of the protocol was performed by re-
22 docking anle138b. The standard comparison of anle138b and our compounds were drawn by
23 comparing their G score values and IFD scores.
24
25

26
27
28 **Statistical Analysis:** All data were analyzed by GraphPad Prism (GraphPad Software) using
29 one-way analysis of variance (ANOVA) with Dunnett's multiple comparison as the post hoc
30 test.
31
32

33 ASSOCIATED CONTENT

34 Supporting Information:

35 The Supporting Information is available free of charge at

36 <https://pubs.acs.org/doi/>

37 The copy of scanned NMR (¹H and ¹³C) spectra and molecular modelling data.

38 Corresponding Author

39 * s.rudrawar@griffith.edu.au

40 * g.mellick@griffith.edu.au

41 Author Contributions

42 S.R. and P.R. conceived and designed the research, P.R. and M.X., performed experimental
43 work and contributed to data analysis and interpretation. K.J. is involved in the molecular
44
45
46
47
48
49
50
51
52
53
54
55
56
57
58
59
60

1
2
3 modelling work. All authors contributed in writing, reviewing and the revision of the
4 manuscript.
5

6 **Funding**

7
8 Financial support to S.R. from an Australian Research Council - Discovery Early Career
9 Research Award (ARC DECRA: DE140101632) is gratefully acknowledged. P.R. received
10 Griffith University Postgraduate Research Scholarship (GUPRS). This work is supported by
11 Menzies Health Institute Queensland (MHIQ), Griffith University Collaborative
12 Interdisciplinary Grants.
13
14
15

16 **Acknowledgements**

17
18 P.R. is supported by Griffith University Postgraduate Research Scholarship.
19

20 **References**

- 21
22 (1) Ryan, P., Xu, M., Davey, A. K., Danon, J. J., Mellick, G. D., Kassiou, M., and Rudrawar,
23 S. (2019) *O*-GlcNAc modification protects against protein misfolding and aggregation in
24 neurodegenerative disease, *ACS Chem. Neurosci.* *10*, 2209-2221.
25
26 (2) Gadad, B. S., Britton, G. B., and Rao, K. S. (2011) Targeting oligomers in
27 neurodegenerative disorders: lessons from alpha-synuclein, tau, and amyloid-beta peptide, *J.*
28 *Alzheimers Dis.* *24 Suppl 2*, 223-232.
29
30 (3) Ryan, P., Patel, B., Makwana, V., Jadhav, H. R., Kiefel, M., Davey, A., Reekie, T. A.,
31 Rudrawar, S., and Kassiou, M. (2018) Peptides, peptidomimetics, and carbohydrate-peptide
32 conjugates as amyloidogenic aggregation inhibitors for Alzheimer's disease, *ACS Chem.*
33 *Neurosci.* *9*, 1530-1551.
34
35 (4) Wagner, J., Ryazanov, S., Leonov, A., Levin, J., Shi, S., Schmidt, F., Prix, C., Pan-Montojo,
36 F., Bertsch, U., Mitteregger-Kretschmar, G., Geissen, M., Eiden, M., Leidel, F., Hirschberger,
37 T., Deeg, A. A., Krauth, J. J., Zinth, W., Tavan, P., Pilger, J., Zweckstetter, M., Frank, T., Bähr,
38 M., Weishaupt, J. H., Uhr, M., Urlaub, H., Teichmann, U., Samwer, M., Bötzel, K., Groschup,
39 M., Kretschmar, H., Griesinger, C., and Giese, A. (2013) Anle138b: a novel oligomer
40 modulator for disease-modifying therapy of neurodegenerative diseases such as prion and
41 Parkinson's disease, *Acta Neuropathol.* *125*, 795-813.
42
43 (5) Levin, J., Schmidt, F., Boehm, C., Prix, C., Bötzel, K., Ryazanov, S., Leonov, A.,
44 Griesinger, C., and Giese, A. (2014) The oligomer modulator anle138b inhibits disease
45 progression in a Parkinson mouse model even with treatment started after disease onset, *Acta*
46 *Neuropathol.* *127*, 779-780.
47
48 (6) Wagner, J., Krauss, S., Shi, S., Ryazanov, S., Steffen, J., Miklitz, C., Leonov, A.,
49 Kleinknecht, A., Goricke, B., Weishaupt, J. H., Weckbecker, D., Reiner, A. M., Zinth, W.,
50
51
52
53
54
55
56
57
58
59
60

1
2
3
4
5
6
7
8
9
10
11
12
13
14
15
16
17
18
19
20
21
22
23
24
25
26
27
28
29
30
31
32
33
34
35
36
37
38
39
40
41
42
43
44
45
46
47
48
49
50
51
52
53
54
55
56
57
58
59
60

Levin, J., Ehninger, D., Remy, S., Kretzschmar, H. A., Griesinger, C., Giese, A., and Fuhrmann, M. (2015) Reducing tau aggregates with anle138b delays disease progression in a mouse model of tauopathies, *Acta Neuropathol.* *130*, 619-631.

(7) Martinez Hernandez, A., Urbanke, H., Gillman, A. L., Lee, J., Ryazanov, S., Agbemeyah, H. Y., Benito, E., Jain, G., Kaurani, L., Grigorian, G., Leonov, A., Rezaei-Ghaleh, N., Wilken, P., Arce, F. T., Wagner, J., Fuhrman, M., Caruana, M., Camilleri, A., Vassallo, N., Zweckstetter, M., Benz, R., Giese, A., Schneider, A., Korte, M., Lal, R., Griesinger, C., Fischer, A., and Eichele, G. (2018) The diphenylpyrazole compound anle138b blocks Abeta channels and rescues disease phenotypes in a mouse model for amyloid pathology, *EMBO Mol. Med.* *10*, 32-47.

(8) Heras-Garvin, A., Weckbecker, D., Ryazanov, S., Leonov, A., Griesinger, C., Giese, A., Wenning, G. K., and Stefanova, N. (2019) Anle138b modulates alpha-synuclein oligomerization and prevents motor decline and neurodegeneration in a mouse model of multiple system atrophy, *Mov. Disord.* *34*, 255-263.

(9) Matthes, D., Gapsys, V., Griesinger, C., and de Groot, B. L. (2017) Resolving the atomistic modes of anle138b inhibitory action on peptide oligomer formation, *ACS Chem. Neurosci.* *8*, 2791-2808.

(10) Kroth, H., Sreenivasachary, N., Hamel, A., Benderitter, P., Varisco, Y., Giriens, V., Paganetti, P., Froestl, W., Pfeifer, A., and Muhs, A. (2016) Synthesis and structure–activity relationship of 2,6-disubstituted pyridine derivatives as inhibitors of β -amyloid-42 aggregation, *Bioorg. Med. Chem. Lett.* *26*, 3330-3335.

(11) Sreenivasachary, N., Kroth, H., Benderitter, P., Hamel, A., Varisco, Y., Hickman, D. T., Froestl, W., Pfeifer, A., and Muhs, A. (2017) Discovery and characterization of novel indole and 7-azaindole derivatives as inhibitors of beta-amyloid-42 aggregation for the treatment of Alzheimer's disease, *Bioorg. Med. Chem. Lett.* *27*, 1405-1411.

(12) Hsieh, C.-J., Xu, K., Lee, I., Graham, T. J. A., Tu, Z., Dhavale, D., Kotzbauer, P., and Mach, R. H. (2018) Chalcones and five-membered heterocyclic isosteres bind to alpha synuclein fibrils *in vitro*, *ACS Omega* *3*, 4486-4493.

(13) Wang, W., and Weisz, K. (2007) Characterization of peptide-pyrazole interactions in solution by low-temperature NMR studies, *Chemistry (Weinheim an der Bergstrasse, Germany)* *13*, 854-861.

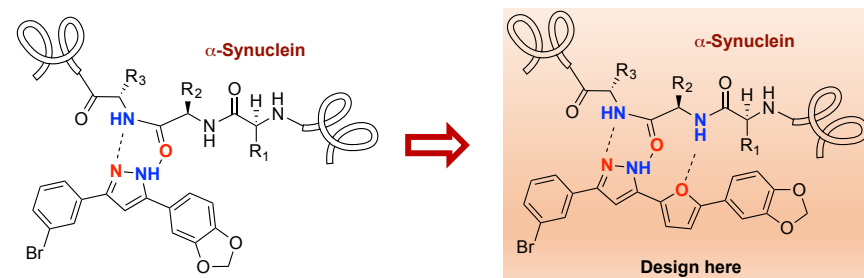
(14) Fricke, H., Gerlach, A., Unterberg, C., Wehner, M., Schrader, T., and Gerhards, M. (2009) Interactions of small protected peptides with aminopyrazole derivatives: the efficiency of blocking a β -sheet model in the gas phase, *Angew. Chem. Int. Ed.* *48*, 900-904.

- 1
2
3 (15) Rzepecki, P., and Schrader, T. (2005) beta-Sheet ligands in action: KLVFF recognition by
4 aminopyrazole hybrid receptors in water, *J. Am. Chem. Soc.* *127*, 3016-3025.
5
6 (16) Rankovic, Z. (2017) CNS physicochemical property space shaped by a diverse set of
7 molecules with experimentally determined exposure in the mouse brain, *J. Med. Chem.* *60*,
8 5943-5954.
9
10 (17) Xu, M., Loa-Kum-Cheung, W., Zhang, H., Quinn, R. J., and Mellick, G. D. (2019)
11 Identification of a new α -synuclein aggregation inhibitor *via* mass spectrometry based
12 screening, *ACS Chem. Neurosci.* *10*, 2683-2691.
13
14 (18) Waxman, E. A.; Giasson, B. I. (2011) Induction of intracellular tau aggregation is
15 promoted by α -synuclein seeds and provides novel insights into the hyperphosphorylation of
16 tau, *J. Neurosci.* *31*, 7604-7618.
17
18 (19) Jha, N. N., Ghosh, D., Das, S., Anoop, A., Jacob, R. S., Singh, P. K., Ayyagari, N.,
19 Namboothiri, I. N. N., and Maji, S. K. (2016) Effect of curcumin analogs on α -synuclein
20 aggregation and cytotoxicity, *Sci. Rep.* *6*, 28511.
21
22 (20) Patel, B., Zunk, D. M., Grant, D. G., and Rudrawar, S. (2018) Solid-phase microwave-
23 assisted ligand-free Suzuki-Miyaura cross-coupling of 5-iodouridine, *ChemistrySelect* *3*, 3187-
24 3193.
25
26 (21) Bhagat, S., Sharma, R., Sawant, D. M., Sharma, L., and Chakraborti, A. K. (2006)
27 LiOH·H₂O as a novel dual activation catalyst for highly efficient and easy synthesis of 1,3-
28 diaryl-2-propenones by Claisen–Schmidt condensation under mild conditions, *J. Mol. Catal.*
29 *A: Chem.* *244*, 20-24.
30
31 (22) Venkatesan, P., and Sumathi, S. (2010) Piperidine mediated synthesis of n-heterocyclic
32 chalcones and their antibacterial activity, *J. Heterocycl. Chem.* *47*, 81-84.
33
34 (23) Bashary, R., and Khatik, G. L. (2019) Design, and facile synthesis of 1,3 diaryl-3-
35 (arylamino)propan-1-one derivatives as the potential alpha-amylase inhibitors and
36 antioxidants, *Bioorg. Chem.* *82*, 156-162.
37
38 (24) Mellado, M., Madrid, A., Reyna, M., Weinstein-Opppenheimer, C., Mella, J., Salas, C. O.,
39 Sánchez, E., and Cuellar, M. (2018) Synthesis of chalcones with antiproliferative activity on
40 the SH-SY5Y neuroblastoma cell line: Quantitative Structure–Activity Relationship Models,
41 *Med. Chem. Res.* *27*, 2414-2425.
42
43 (25) Buriol, L., Frizzo, C. P., Marzari, M. R. B., Moreira, D. N., Prola, L. D. T., Zanatta, N.,
44 Bonacorso, H. G., and Martins, M. A. P. (2010) Pyrazole synthesis under microwave irradiation
45 and solvent-free conditions, *J. Braz. Chem. Soc.* *21*, 1037-1044.
46
47
48
49
50
51
52
53
54
55
56
57
58
59
60

- 1
2
3
4 (26) Coelho-Cerqueira, E., Pinheiro, A. S., and Follmer, C. (2014) Pitfalls associated with the
5 use of Thioflavin-T to monitor anti-fibrillogenic activity, *Bioorg. Med. Chem. Lett.* *24*, 3194-
6 3198.
7
8 (27) Lassen, L. B., Gregersen, E., Isager, A. K., Betzer, C., Kofoed, R. H., and Jensen, P. H.
9 (2018) ELISA method to detect α -synuclein oligomers in cell and animal models, *PLoS One*
10 *13*, e0196056-e0196056.
11
12 (28) Masuda, M., Hasegawa, M., Nonaka, T., Oikawa, T., Yonetani, M., Yamaguchi, Y., Kato,
13 K., Hisanaga, S.-i., and Goedert, M. (2009) Inhibition of α -synuclein fibril assembly by small
14 molecules: Analysis using epitope-specific antibodies, *FEBS Lett.* *583*, 787-791.
15
16 (29) Lassen, L.B.; Gregersen, E.; Isager, A. K.; Betzer, C.; Kofoed, R. H.; Jensen, P. H. (2018)
17 ELISA method to detect α -synuclein oligomers in cell and animal models, *PLoS One* *13*,
18 e0196056.
19
20 (30) Masuda, M.; Hasegawa, M.; Nonaka, T.; Oikawa, T.; Yonetani, M.; Yamaguchi, Y.;
21 Kato, K.; Hisanaga, S.-I.; Goedert, M. (2009) Inhibition of α -synuclein fibril assembly by
22 small molecules: analysis using epitope-specific antibodies, *FEBS Lett.* *583*, 787-791.
23
24 (31) Friesner, R. A.; Murphy, R. B.; Repasky, M. P.; Frye, L. L.; Greenwood, J. R.; Halgren, T.
25 A.; Sanschagrín, P. C.; Mainz, D. T. (2006) Extra precision Glide: docking and scoring
26 incorporating a model of hydrophobic enclosure for protein-ligand complexes, *J. Med. Chem.*
27 *49*, 6177-6196.
28
29 (32) Halgren, T. A.; Murphy, R. B.; Friesner, R. A.; Beard, H. S.; Frye, L. L.; Pollard, W. T.;
30 Banks, J. L. (2004) Glide: a new approach for rapid, accurate docking and scoring 2.
31 Enrichment factors in database screening, *J. Med. Chem.* *47*, 1750-1759.
32
33 (33) Sherman, W.; Day, T.; Jacobson, M. P.; Friesner, R. A.; Farid, R. (2006) Novel procedure
34 for modeling ligand/receptor induced fit effects, *J. Med. Chem.* *49*, 534-553;
35
36 (34) Sherman, W.; Beard, H. S.; Farid, R. (2006) Use of an induced fit receptor structure in
37 virtual screening, *Chem. Biol. Drug Des.*, *67*, 83-84.
38
39 (35) Li, J.; Abel, R.; Zhu, K.; Cao, Y.; Zhao, S.; Friesner, R. A. (2011) The VSGB 2.0 model:
40 a next generation energy model for high resolution protein structure modeling, *Proteins*, *79*,
41 2794-812
42
43 (36) Volles, M. J., and Lansbury, P. T., Jr. (2007) Relationships between the sequence of alpha-
44 synuclein and its membrane affinity, fibrillization propensity, and yeast toxicity, *J. Mol. Biol.*
45 *366*, 1510-1522.
46
47
48
49
50
51
52
53
54
55
56
57
58
59
60

- 1
2
3 (37) Pujols, J., Peña-Díaz, S., Conde-Giménez, M., Pinheiro, F., Navarro, S., Sancho, J., and
4 Ventura, S. (2017) High-throughput screening methodology to identify alpha-synuclein
5 aggregation inhibitors, *Int. J. Mol. Sci.* *18*, E478.
6
7
8 (38) Rahimi, F., Maiti, P., and Bitan, G. (2009) Photo-induced cross-linking of unmodified
9 proteins (PICUP) applied to amyloidogenic peptides, *J. Vis. Exp.* *23*, 1071.
10
11 (39) Liu, Y.; Fallon, L.; Lashuel, H. A.; Liu, Z.; Lansbury, P. T. Jr. (2002) The UCH-L1 gene
12 encodes two opposing enzymatic activities that affect alpha-synuclein degradation and
13 Parkinson's disease susceptibility. *Cell* *111*, 209-218.
14
15 (40) Ham, S.; Kim, H.; Hwang, S.; Kang, H.; Yun, S. P.; Kim, S.; Kim, D.; Kwon, H. S.; Lee,
16 Y.-S.; Cho, M. L.; Shin, H.-M.; Choi, H.; Chung, K. Y.; Ko, H. S.; Lee, G. H.; Lee, Y. (2019)
17 Cell-based screen using amyloid mimic β 23 expression identifies peucedanocoumarin III as a
18 novel inhibitor of α -synuclein and Huntingtin aggregates. *Mol Cells* *42*, 480-494.
19
20 (41) Friesner, R. A.; Banks, J. L.; Murphy, R. B.; Halgren, T. A.; Klicic, J. J.; Mainz, D. T.;
21 Repasky, M. P.; Knoll, E. H.; Shaw, D. E.; Shelley, M.; Perry, J. K.; Francis, P.; Shenkin, P.
22 S. (2004) Glide: a new approach for rapid, accurate docking and scoring. 1. Method and
23 assessment of docking accuracy, *J. Med. Chem.* *47*, 1739-1749.
24
25 (42) Harder, E.; Damm, W.; Maple, J.; Wu, C.; Reboul, M.; Xiang, J.Y.; Wang, L.; Lupyran,
26 D.; Dahlgren, M.K.; Knight, J.L.; Kaus, J.W.; Cerutti, D.S.; Krilov, G.; Jorgensen, W.L.; Abel,
27 R.; Friesner, R.A. (2016) OPLS3: A force field providing broad coverage of drug-like small
28 molecules and proteins, *J. Chem. Theory Comput.* *12*, 281-296.
29
30 (43) Halgren, T. (2007) New method for fast and accurate binding-site identification and
31 analysis, *Chem. Biol. Drug Des.* *69*, 146-148.
32
33
34
35
36
37
38
39
40
41
42
43
44
45
46
47
48
49
50
51
52
53
54
55
56
57
58
59
60

Table of Contents - Abstract Graphics



Pre-clinical candidate anle138b

